

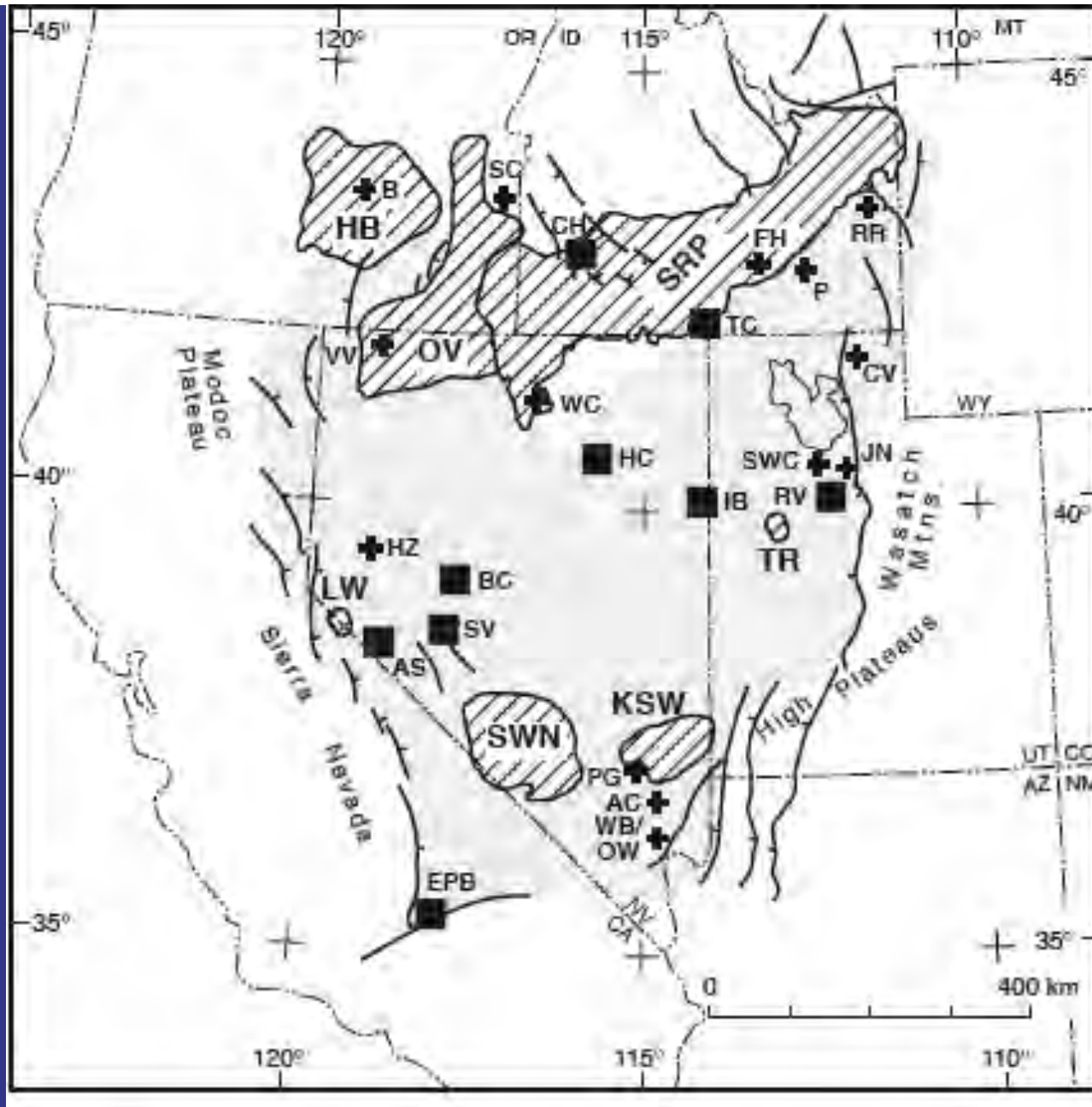


RATTLESNAKES

RATTLESNAKES MAY BE FOUND IN THIS AREA.

**THEY ARE IMPORTANT MEMBERS OF THE
NATURAL COMMUNITY. THEY WILL NOT
ATTACK, BUT IF DISTURBED OR CORNERED,
THEY WILL DEFEND THEMSELVES.**

GIVE THEM DISTANCE AND RESPECT.

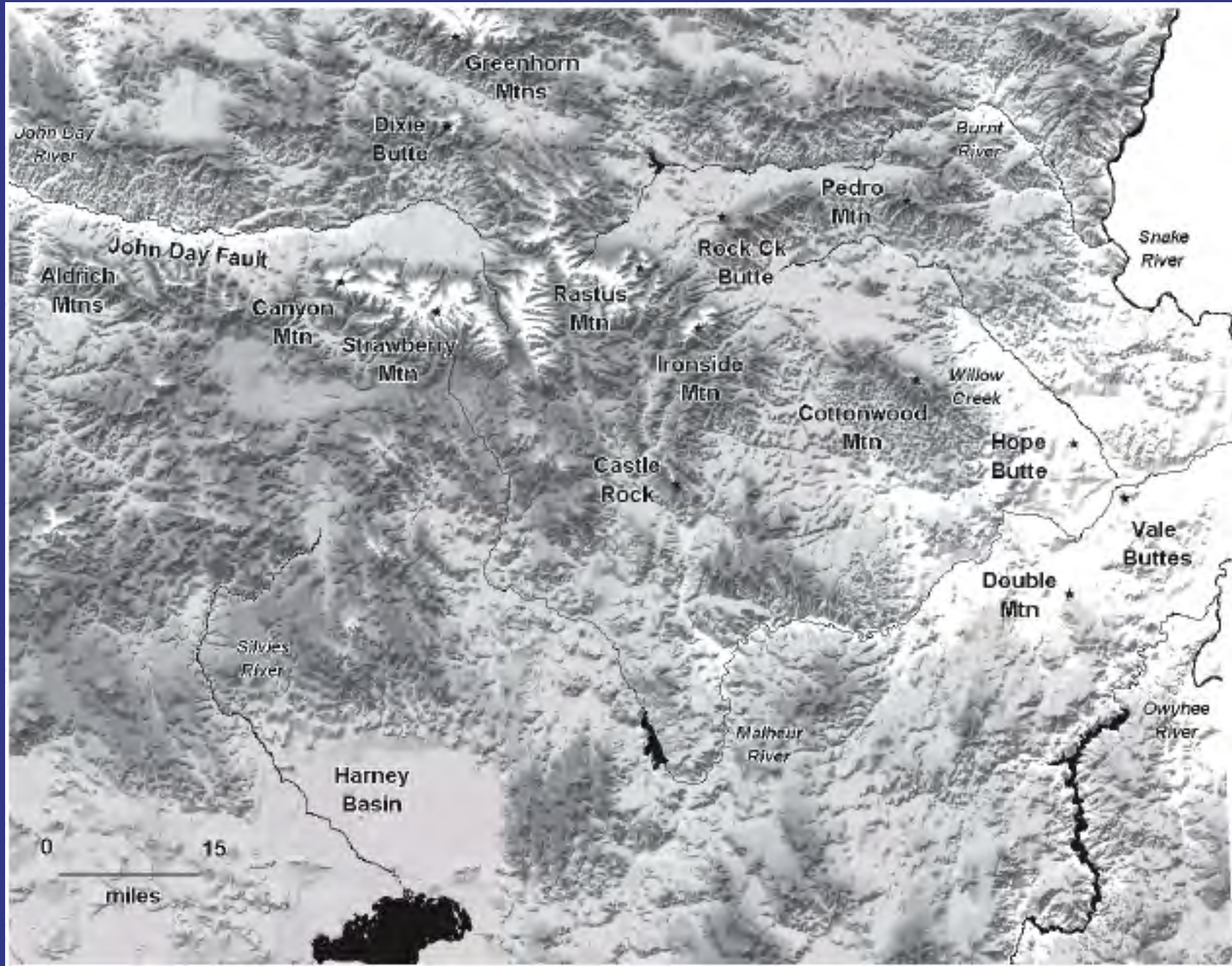


Miocene Silicic Volcanic Centers

Streck and Ferns (2004)

The Rattlesnake Tuff and
other Miocene silicic
volcanism in Eastern Oregon

Field Trip Guide
2004 GSA Cordilleran
Meeting



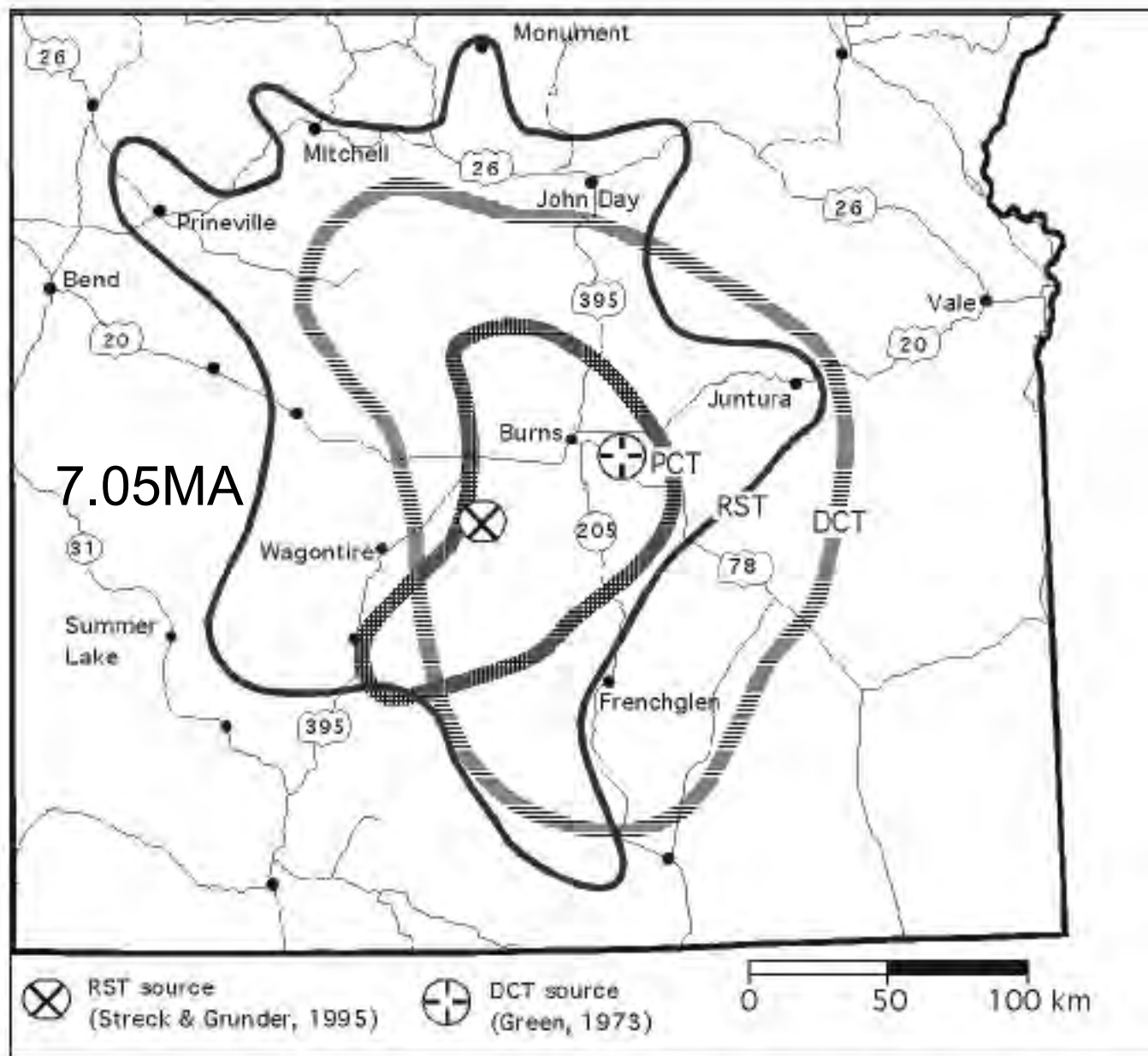


Figure 4. Inferred outlines and source areas of Harney Basin Tuffs. RST, Rattlesnake Tuff; PCT, Prater Creek Tuff; DCT, Devine Canyon Tuff. Outlines for DCT and PCT modified from Green (1973) and Walker (1979), respectively.

Some vocabulary:

Tuff: volcanic rock formed from fragments < 4 mm

Welded tuff: tuff that is indurated by heat and gas

Spherulites: small, radiating, concentric minerals in a spherical shape, often found in silicic rocks or obsidians

Lithophysae: spherulites found in rhyolites, obsidians, etc

Vitric: glassy

Devitrification: process that converts glass to mineral

Perlitic: texture of irregular, concentric, or spheroidal cracks due to contraction during cooling.

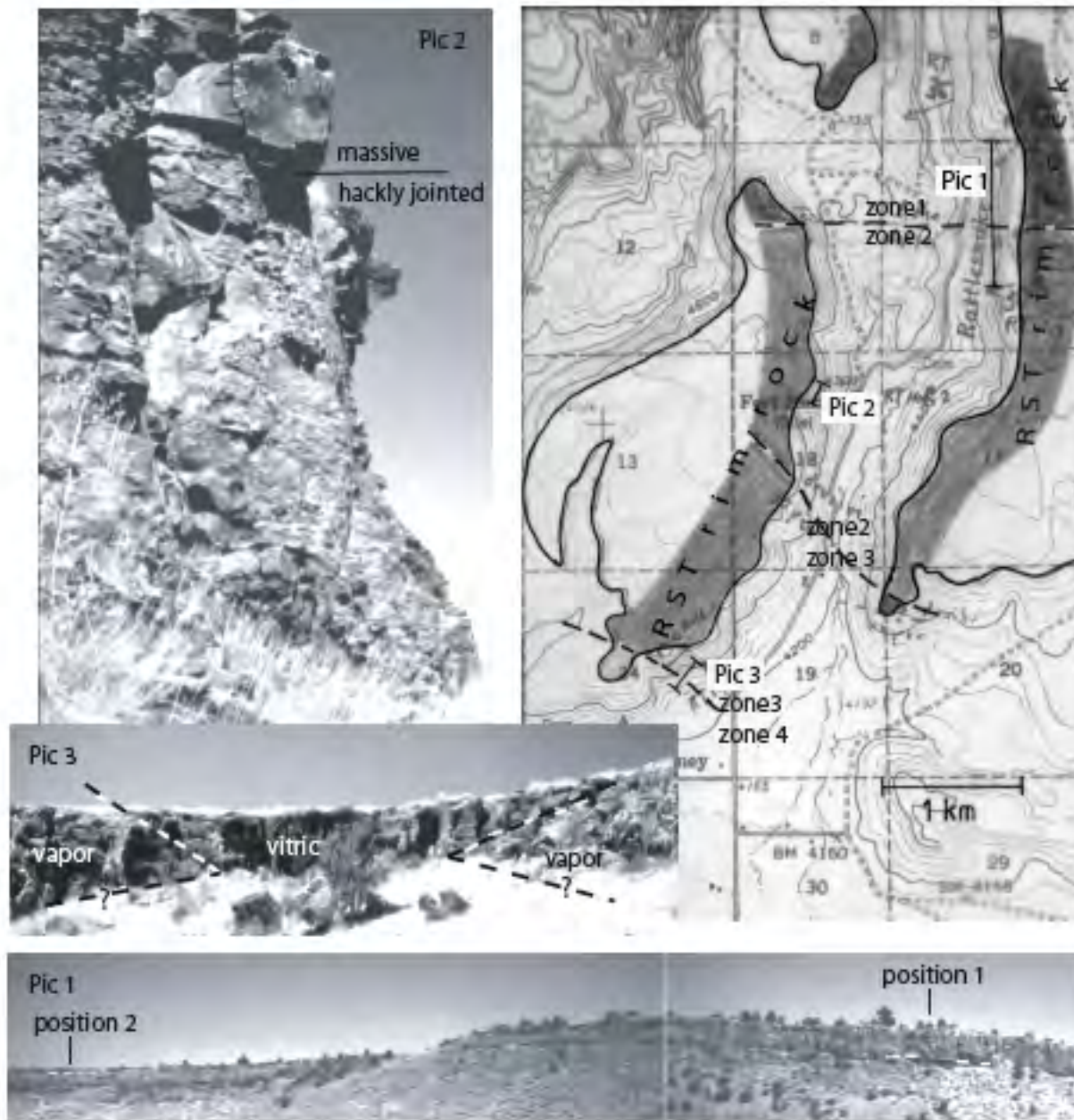


Figure 5. Overview of local facies changes. Zone 1: tuff dominated by thick lithophysal tuff underlying pervasively devitrified tuff and overlying (inferred, not exposed here) lower non- to densely welded vitric tuff. Zone 2: tuff dominated by pervasively devitrified tuff (Pic 2) overlying lower vitric tuff and underlying upper vitric tuff. Zone 3: tuff section consists of partially welded (with pumice) tuff that is vitric or vapor phase altered. Zone 4: vitric incipiently welded tuff. Picture 1: at position 1, densely welded vitrophyre exposed below white dashed line and section is topped with float of upper vitric tuff and at position 2, entire section below white dashed line is lithophysal tuff. Picture 2 shows pervasively devitrified tuff throughout in two facies, hackly jointed and massive. Picture 3: in middle of picture, tuff consists entirely of vitric tuff (vitric) that splits into a lower and upper vitric tuff separated by vapor phase tuff (vapor) further to the right and left, dashed lines indicate position of sharp interfaces between vitric and vapor phase tuff (analogous to the one seen in fig. 13 in Streck and Grunder, 1995).

Rattlesnake Tuff Outcrops

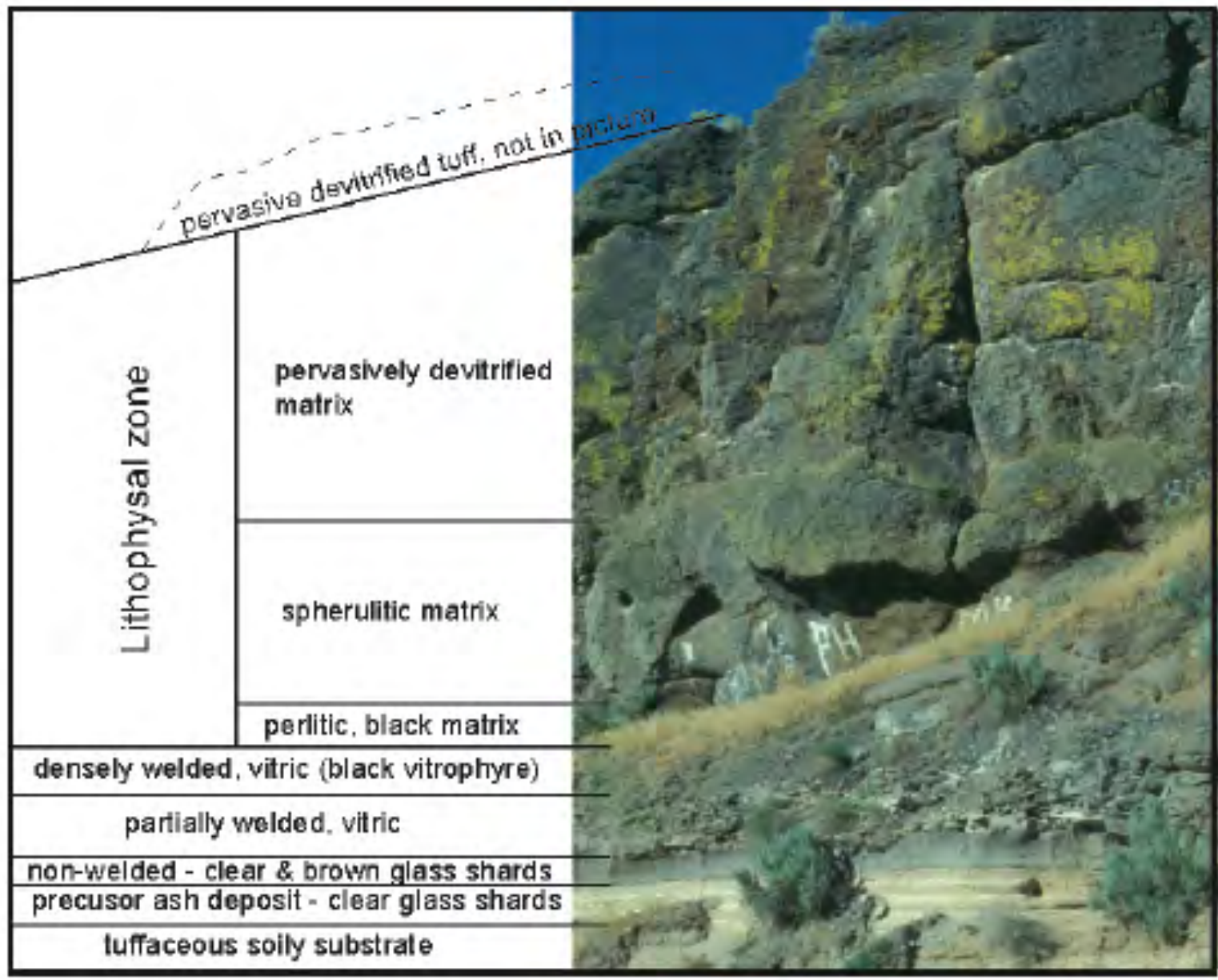


Figure 6. Outcrop stratigraphy of Rattlesnake Tuff at Stop 7.

Type Locality Rattlesnake Tuff

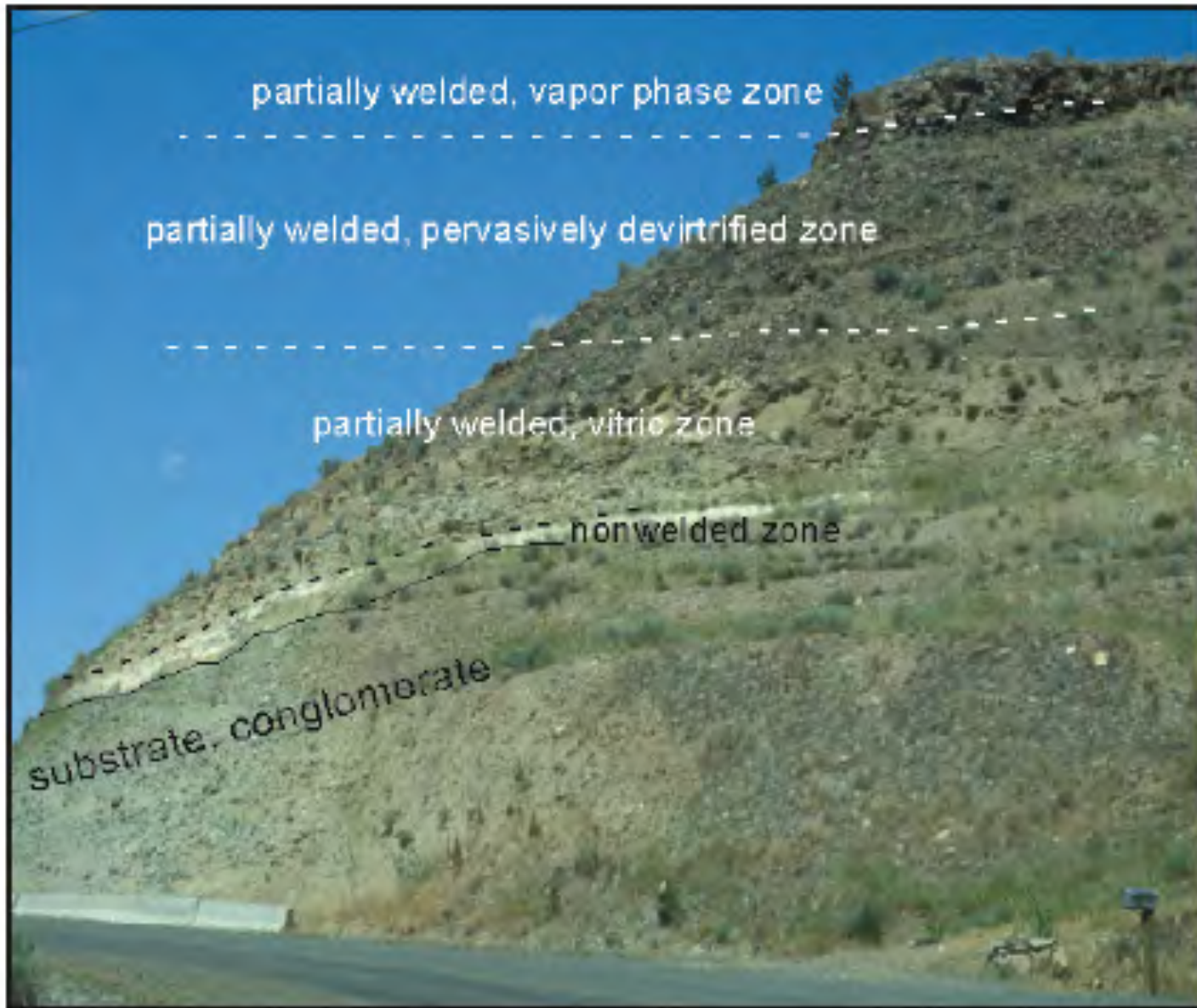


Figure 7. Outcrop stratigraphy of Rattlesnake Tuff at Stop 9.

Distal edge of Rattlesnake Tuff

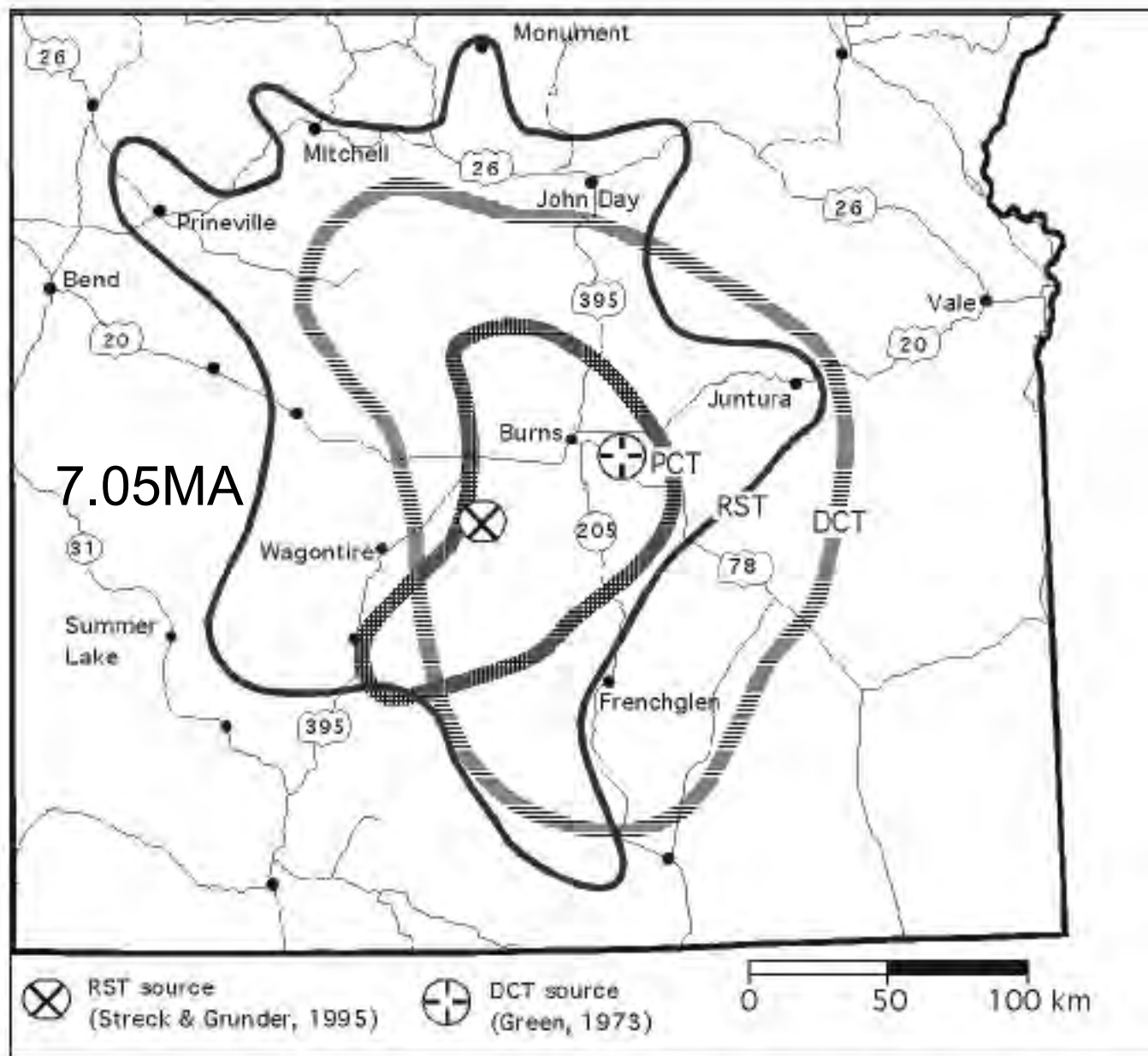


Figure 4. Inferred outlines and source areas of Harney Basin Tuffs. RST, Rattlesnake Tuff; PCT, Prater Creek Tuff; DCT, Devine Canyon Tuff. Outlines for DCT and PCT modified from Green (1973) and Walker (1979), respectively.

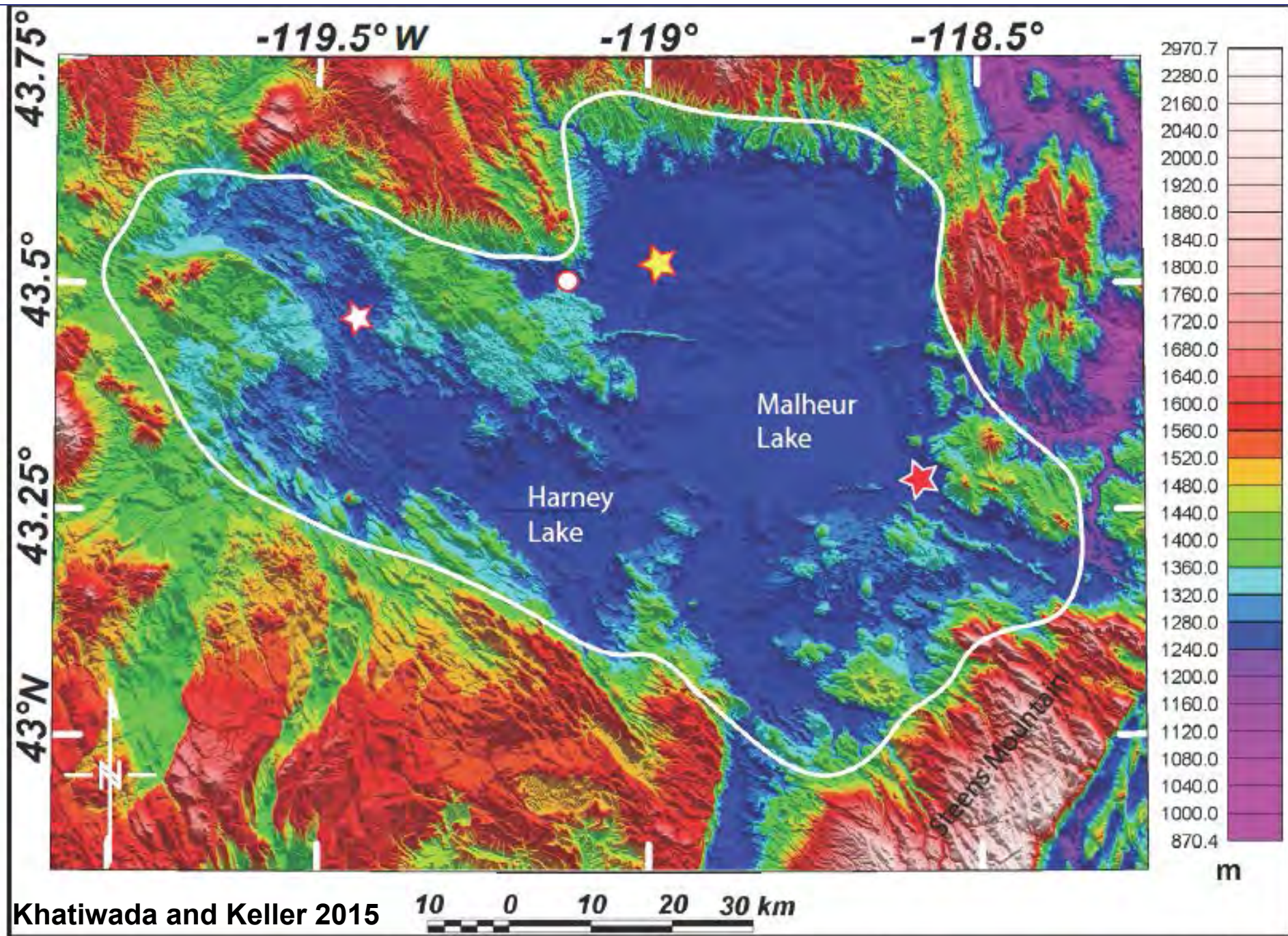


Figure 2. High-resolution (10 m) digital elevation map (DEM) of the Harney Basin area. The white line represents the physiographic bound-

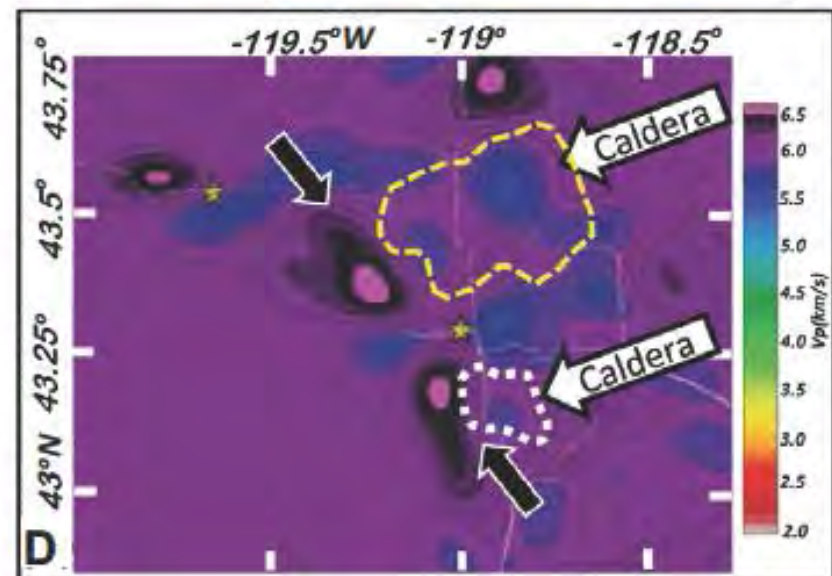
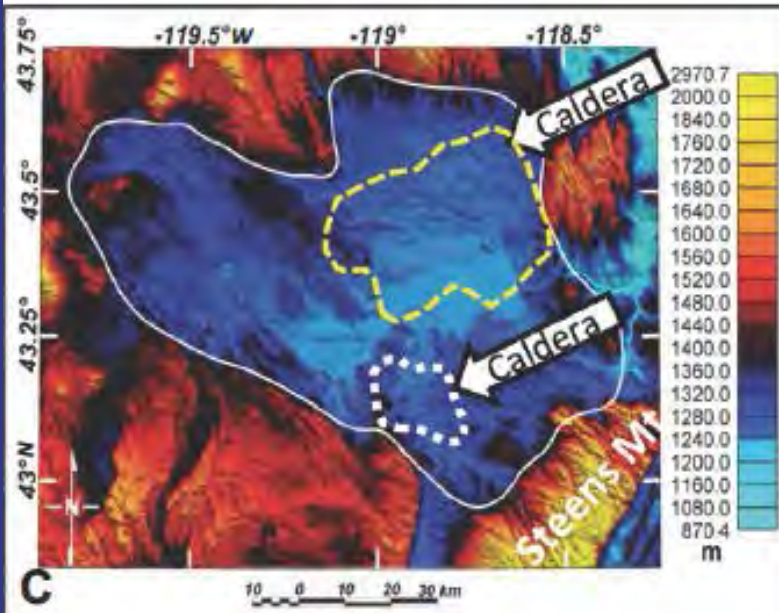
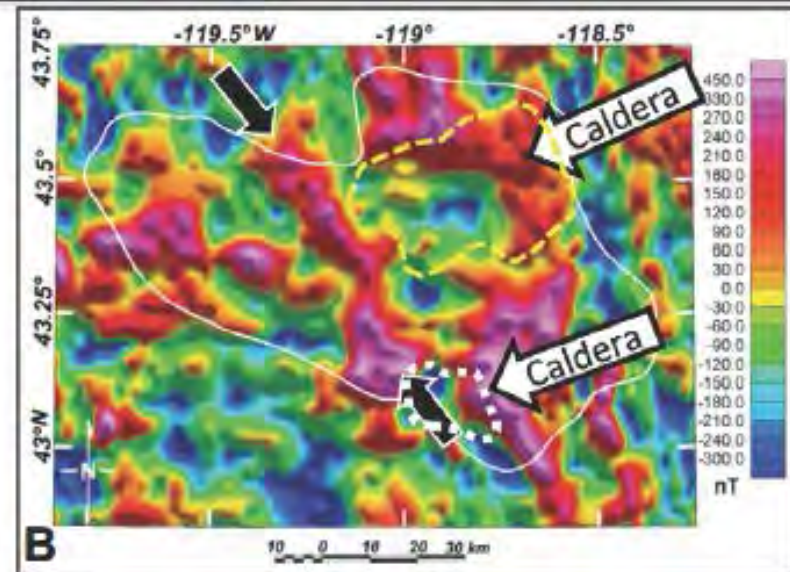
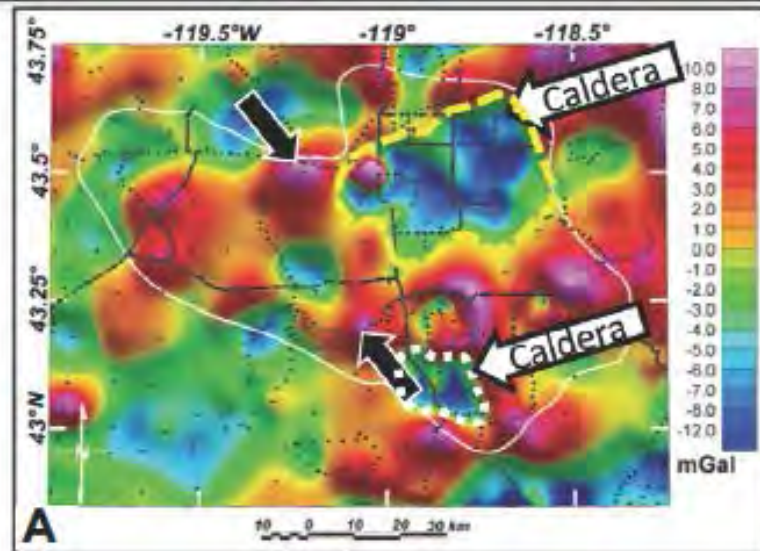
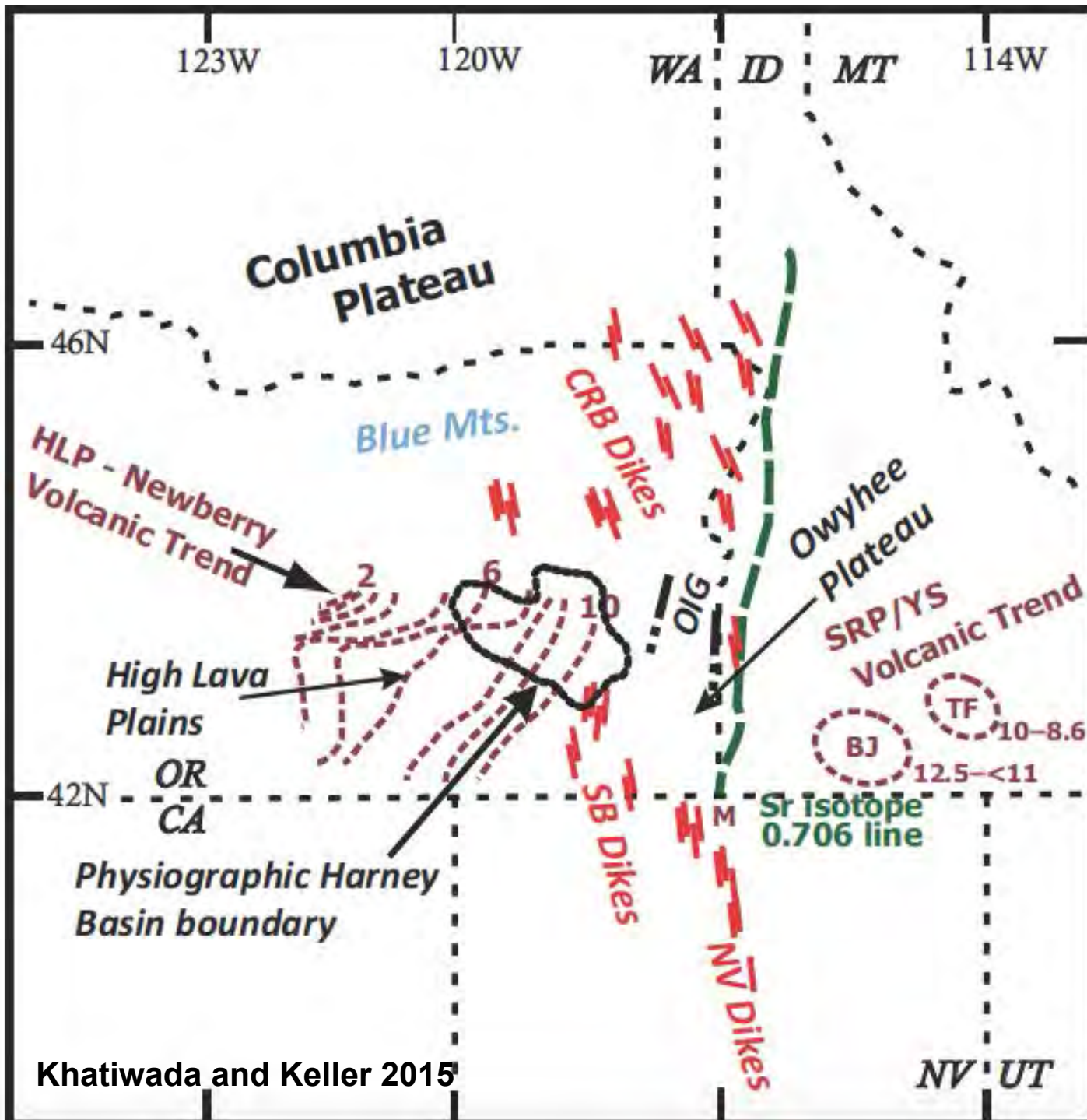


Figure 13. Harney Basin features expressed in multiple data sets: (A) residual complete Bouguer anomaly (CBA) map after 15 km upward continuation; (B) reduced-to-pole total magnetic intensity (TMI) map; (C) 10 m resolution digital elevation model; and (D) seismic-velocity model at 4 km below sea level (bsl). All of these maps suggest the presence of possible calderas (dashed white and yellow lines) in the basin. The pair of black arrows indicate possible mafic dikes. Khatiwada and Keller 2015



Khatiwada and Keller 2015

Miocene Flood Basalts



Beeson et al 1985

SERIES	GROUP	SUB-GROUP	FORMATION	MEMBER	K-Ar AGE (m.y.)	MAGNETIC POLARITY			
MIOCENE	UPPER	COLUMBIA RIVER BASALT GROUP	YAKIMA BASALT SUBGROUP	LOWER MONUMENTAL MEMBER	6	N			
				<i>Erosional Unconformity</i>					
				ICE HARBOR MEMBER	8.5				
				Basalt of Goose Island		N			
				Basalt of Martindale		R			
				Basalt of Basin City		N			
				<i>Erosional Unconformity</i>					
				BUFORD MEMBER		R			
				ELEPHANT MOUNTAIN MEMBER	10.5	R,T			
				<i>Erosional Unconformity</i>					
				POMONA MEMBER	12	R			
				<i>Erosional Unconformity</i>					
				ESQUATZEL MEMBER		N			
				<i>Erosional Unconformity</i>					
				WEISSENFELS RIDGE MEMBER					
	Basalt of Slippery Creek		N						
	Basalt of Lewiston Orchards		N						
	ASOTIN MEMBER		N						
	<i>Local Erosional Unconformity</i>								
	WILBER CREEK MEMBER								
	Basalt of Lapwai		N						
	Basalt of Wahluke		N						
	UMATILLA MEMBER								
	Basalt of Sillusi		N						
	Basalt of Umatilla		N						
	<i>Local Erosional Unconformity</i>								
	PRIEST RAPIDS MEMBER	14.5							
	Basalt of Lolo		R						
	Basalt of Rosalia		R						
	ROZA MEMBER		T,R						
	FRENCHMAN SPRINGS MEMBER								
	Basalt of Lyons Ferry		N						
	Basalt of Sentinel Gap		N						
Basalt of Sand Hollow		N							
Basalt of Silver Falls		N,E							
Basalt of Ginkgo		E							
Basalt of Palouse Falls		N							
ECKLER MOUNTAIN MEMBER									
Basalt of Shumaker Creek		N							
Basalt of Dodge		N							
Basalt of Robinette Mountain		N							
GRANDE RONDE BASALT	15.5 - 16.5	N ₂							
		R ₂							
PICTURE GORGE BASALT	(14.6-15.8)	N ₁							
		R ₁							
IMNAHA BASALT	16.5 - 17.0	R ₁							
		T							
		N ₀							
		R ₀							

Figure 1. Stratigraphic nomenclature, age, and magnetic polarity for the Columbia River Basalt Group, as revised by Swanson and others (1979b) and modified by the authors. N = normal magnetic polarity; R = reversed magnetic polarity; T = transitional magnetic polarity; E = excursions magnetic polarity.

MACKIN (1961, p.8)	BENTLEY (1977a, p.361)	BENTLEY AND CAMPBELL (1983)	THIS PAPER
			BASALT OF LYONS FERRY
SENTINEL GAP FLOW	UNION GAP FLOWS	FLOWS OF UNION GAP	BASALT OF SENTINEL GAP
SAND HOLLOW FLOW	KELLEY HOLLOW FLOWS SAND HOLLOW FLOWS MARY HILL FLOW	FLOW OF KELLEY HOLLOW† FLOW OF BADGER GAP**	BASALT OF SAND HOLLOW* BASALT OF SILVER FALLS
GINKGO FLOW	GINKGO FLOW	GINKGO FLOWS	BASALT OF GINKGO
	PALOUSE FALLS FLOW		BASALT OF PALOUSE FALLS

† Equivalent to the Sand Hollow and Sentinel Gap Flows of Mackin (1961)

** Sand Hollow Flow of Bentley (1977a)

* Includes Basalt of Sheffler (Swanson and others, 1980)

Figure 2. Chart showing correlation of previously defined units of the Frenchman Springs Member to those of this paper.

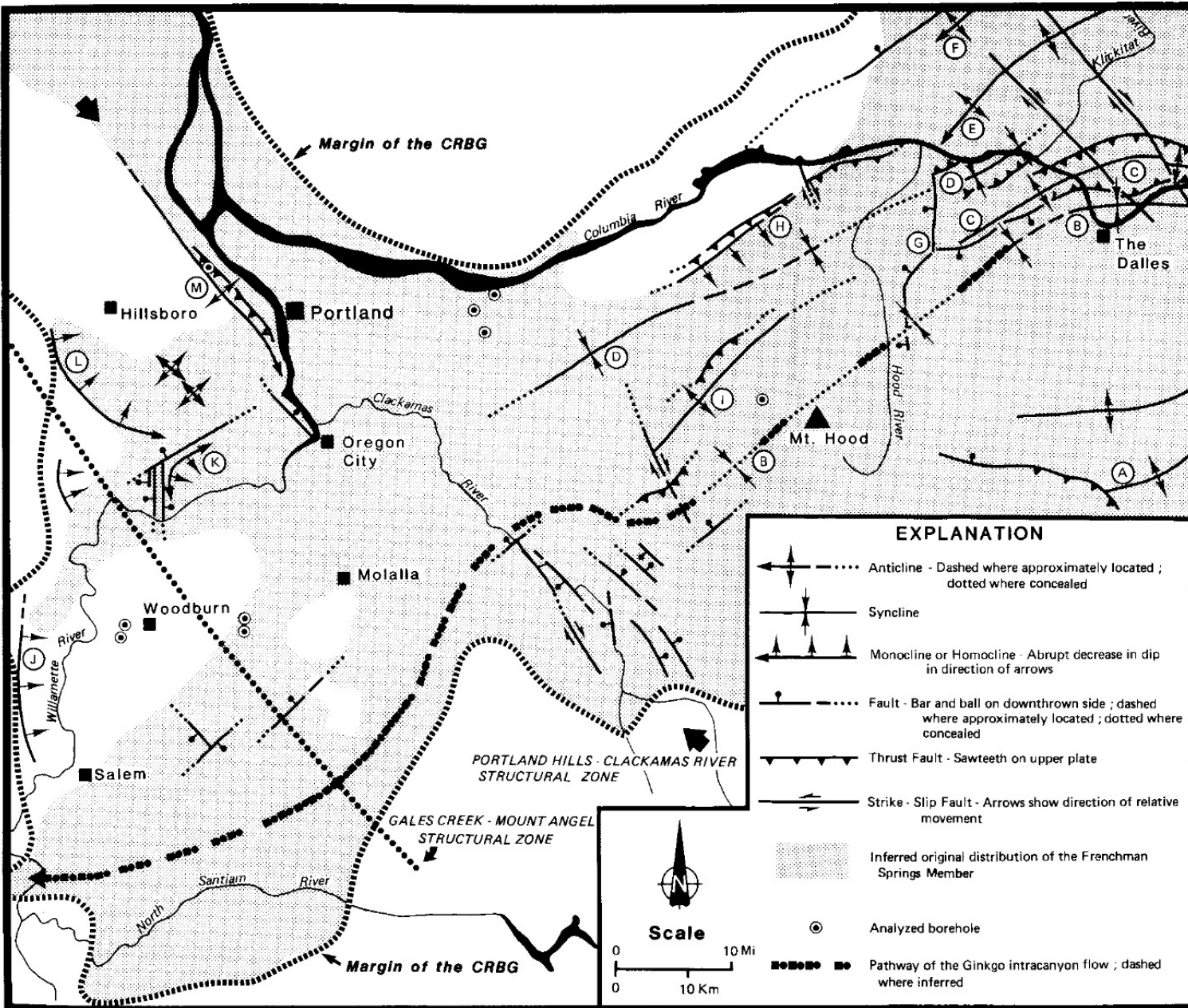


Figure 6. Generalized sketch map showing selected major structures in western Oregon and Washington and the pathway of the Ginkgo intracanyon flow. Structural features shown include the following: A = Tygh Ridge; B = Dalles-Mount Hood syncline; C = Columbia Hills; D = Mosier-Bull Run syncline; E = Bingen anticline; F = Horse Heaven Hills-Simcoe Mountains uplift; G = Hood River fault zone; H = Eagle Creek homocline; I = Bull Run anticline; J = Eola Hills homocline; K = Parrett Mountain structure; L = Chehalem Mountain homocline; M = Portland Hills anticline.

Eastern Oregon Flood Basalts

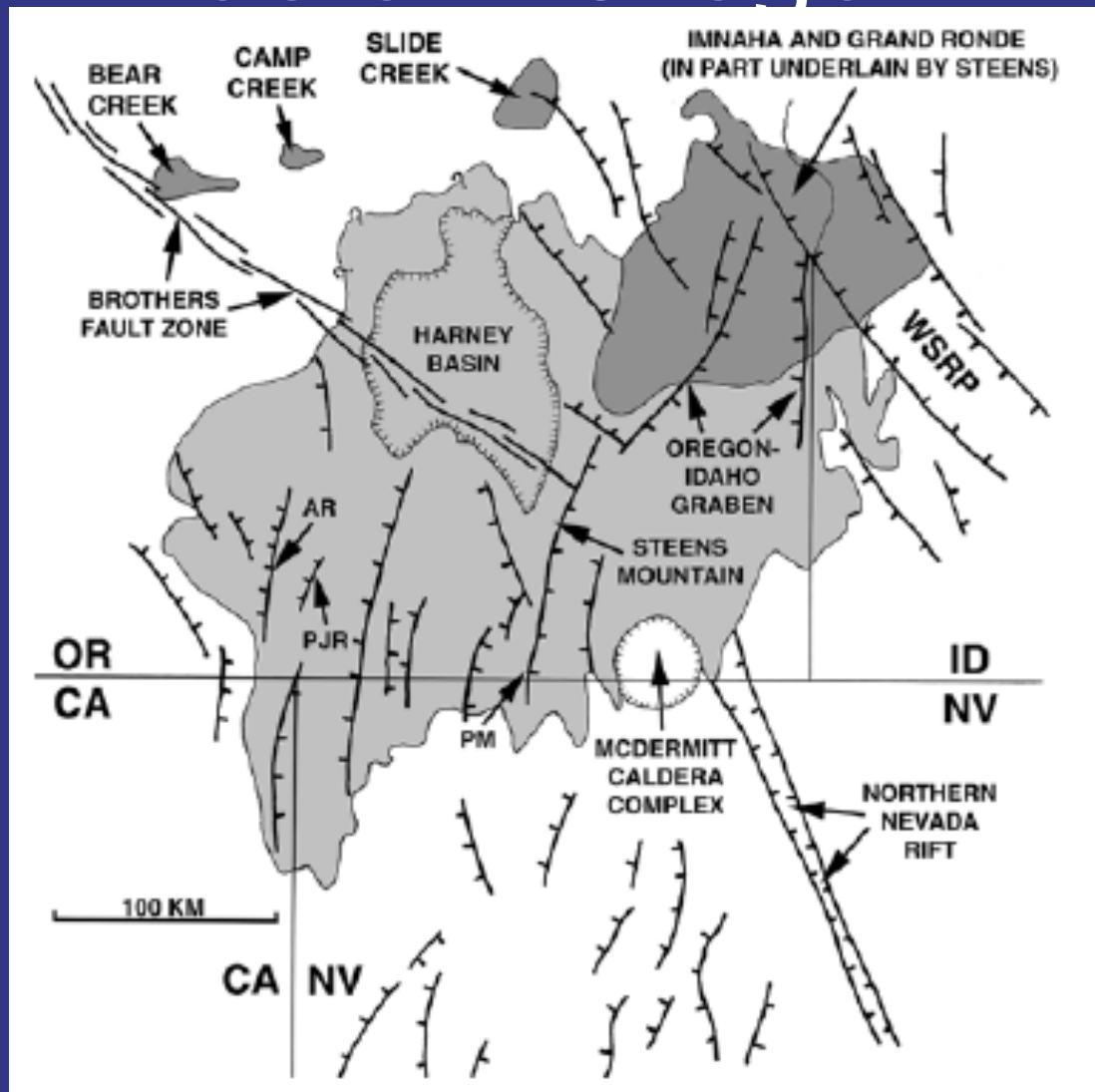


Figure 1. Approximate distribution of Miocene flood basalts in southeastern Oregon (~16.6–15.3 Ma). AR, Abert Rim; PJR, Poker Jim Ridge; PM, Pueblo Mountains, WSRP, Western Snake River Plain. See color version of this

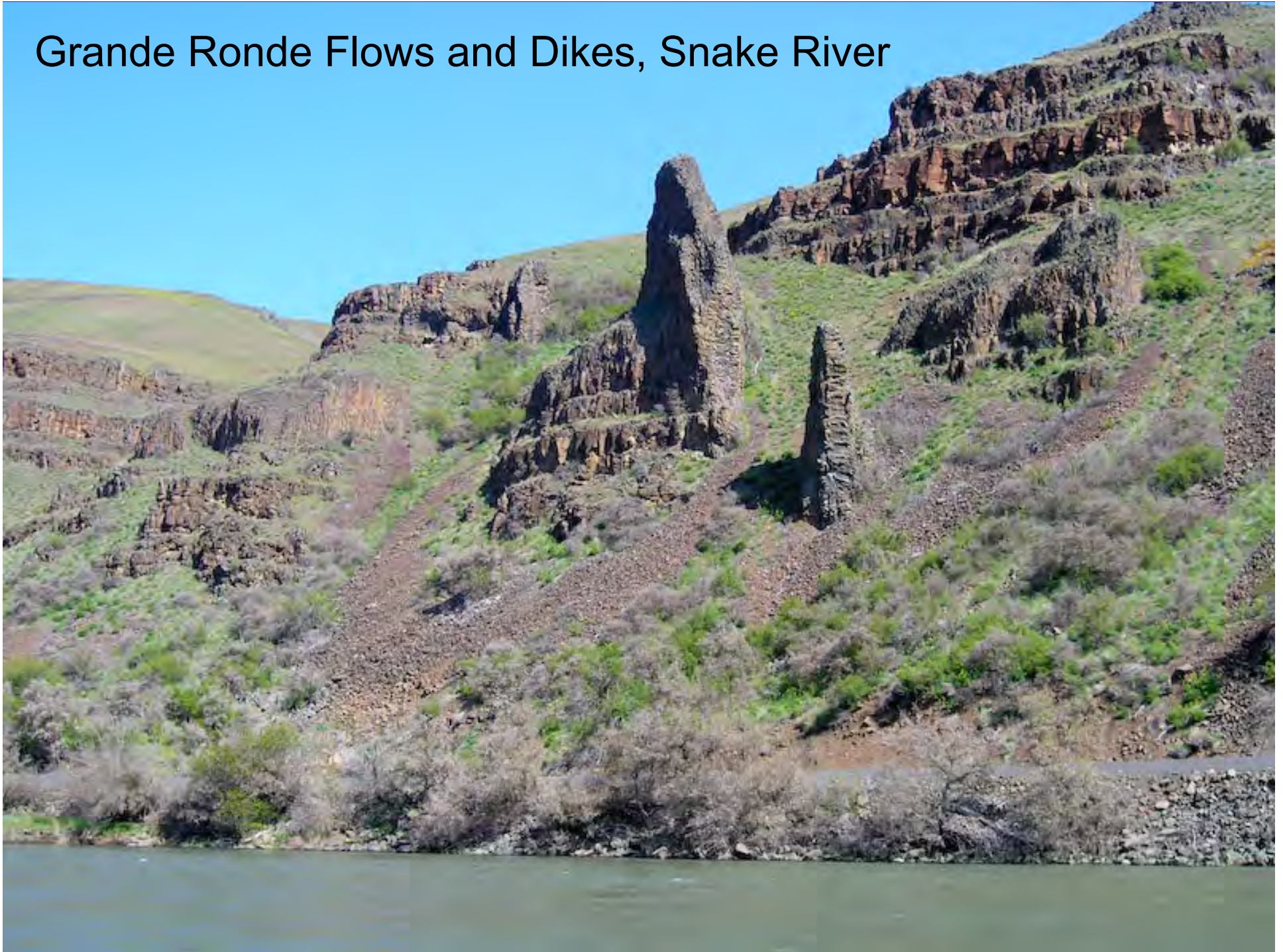


Picture Gorge Basalts from Sheldon (2003)



CRB dikes in Wallow Granite

Grande Ronde Flows and Dikes, Snake River



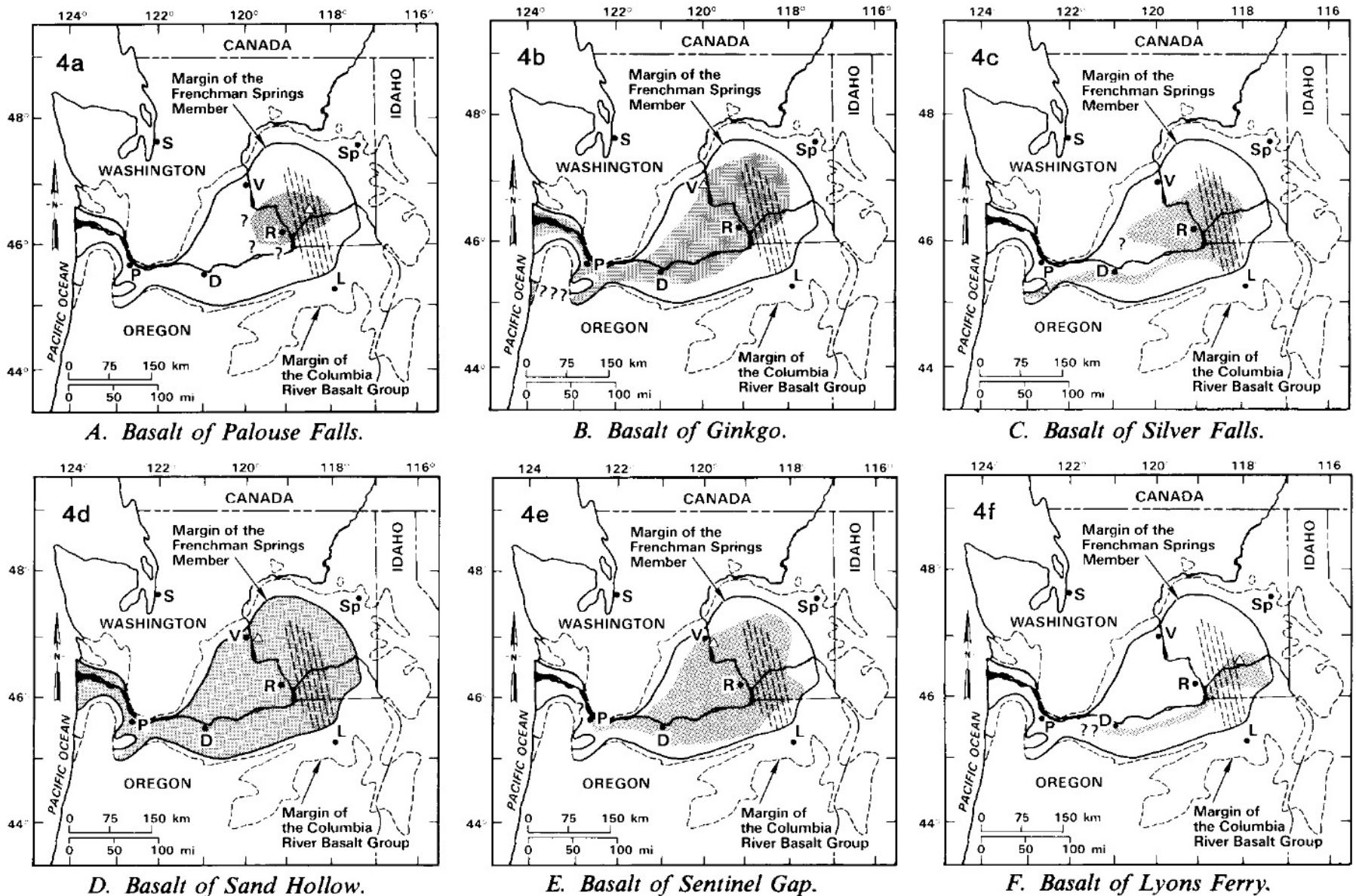
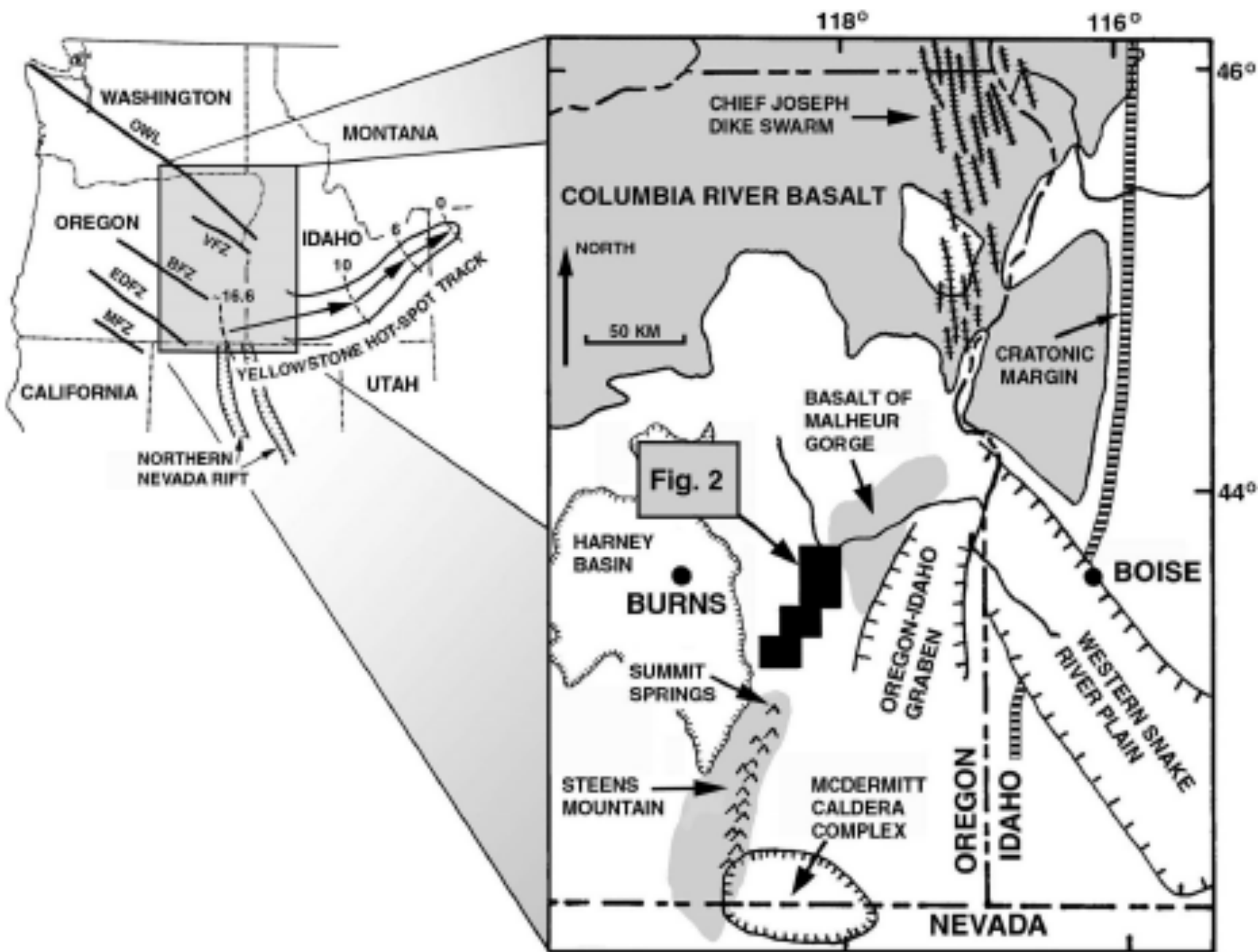


Figure 4. Maps showing inferred original extent (stippled areas) of units of the Frenchman Springs Member defined in this paper. Known and inferred dike and vent areas are shown schematically by parallel dashed lines. Locations of type localities are designated by open triangles. Cities: Sp = Spokane; L = La Grande; R = Richland; V = Vantage; D = The Dalles; S = Seattle; P = Portland.

Genesis of flood basalts ...
from Steens Mountains to the
Malheur River Gorge, Oregon

Camp et al 2003
GSA Bulletin pp. 105-128.



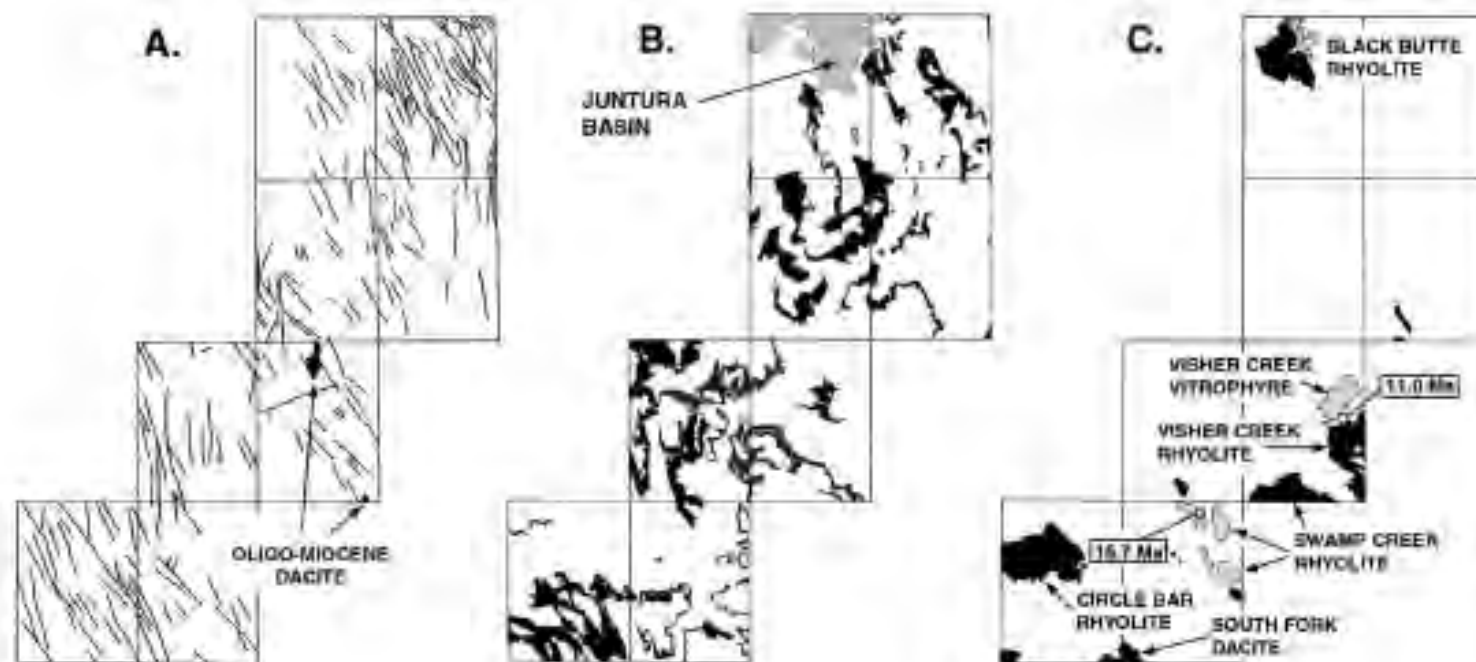


Figure 3. Aspects of the general geology. (A) Overall fault pattern and distribution of the Oligocene–Miocene volcanic rocks. (B) Distribution of the undifferentiated Miocene pyroclastic rocks and pyroclastic sediments, spanning an age range from ca. 15.0 and 7.0 Ma. (C) Distribution of the shallow felsic eruptive centers. Outflow facies of ignimbrite or vitrophyric lava are shown by dotted pattern. Radiometric dates for the Swamp Creek and Visher Creek rhyolites are from Walker (1979).

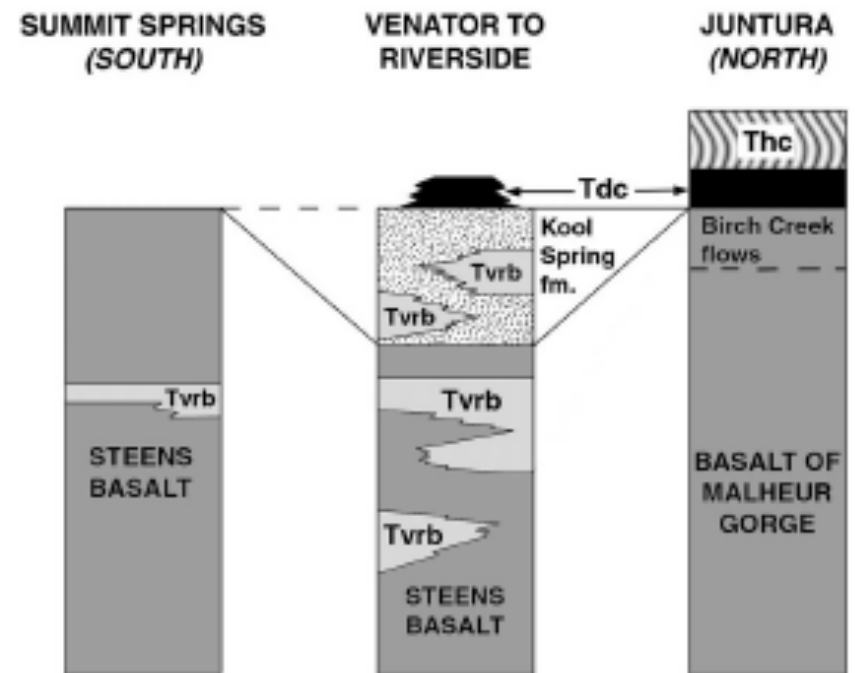
VOLCANIC SUCCESSION	VOLCANIC UNIT	AGE	COMMENT
Late Diaktyaxitic Olivine Basalts <i>Regional Unconformity</i>	Voltage flow	32 ka	A
	Drinkwater basalt	ca. 7.0 Ma	B
Intermediate to Felsic Calc-alkaline Rocks <i>Regional Unconformity</i>	KEENEY SEQUENCE	Devine Canyon tuff	ca. 9.7 Ma
		Cobb Creek lavas	—
		Riverside lavas	10.14 ± 0.23 Ma
		Buck Mtn. lavas	12.5 ± 0.5 Ma
Early Diaktyaxitic Olivine Basalts <i>Regional Unconformity</i>	Tims Peak basalt	13.5 ± 0.1 Ma	F
Tholeiitic Mafic to Bimodal Rocks <i>Regional Unconformity</i>	Hunter Creek basalt	15.3 ± 0.1 Ma	F,G
	Dinner Creek tuff		
	Kool Spring Im.	—	—
	Steens basalt, Venator Ranch basalt, and basalt of Malheur Gorge	15.7 ± 0.1 Ma	F,G
		16.6 ± 0.02 Ma	H
Oligo-Miocene dacite		ca. 23.7-17.8 Ma	I

Volcanic stratigraphy along the middle and south forks of the Malheur River, Oregon, is subdivided by well-developed unconformities. Comments on age designations: (A) Gehr and Newman (1974); (B) Gehr and Newman (1974); (C) Gehr and Newman (1974); (D) Gehr and Newman (1974); (E) Gehr and Newman (1974); (F) Gehr and Newman (1974); (G) Gehr and Newman (1974); (H) Gehr and Newman (1974); (I) Gehr and Newman (1974).



Figure 5. Dike of Venator Ranch basalt cutting across Oligocene–Miocene volcanic rocks in the McEwen Butte Quadrangle, 7 km south of Riverside, Oregon.

LOWER THOLEIITIC TO BIMODAL VOLCANIC ROCKS



in the north. Throughout most of this region, the upper part of the Steens sequence is interbedded with a group of previously unrecognized tholeiitic lavas, herein referred to as the

Venator Ranch basalt. The interbedded succession of Steens and Venator Ranch basalts in turn overlain by an interbedded bimodal succession of air-fall pyroclastic deposits and Venator Ranch basalt flows, herein called the Kool Spring formation (Figs. 4). Two small

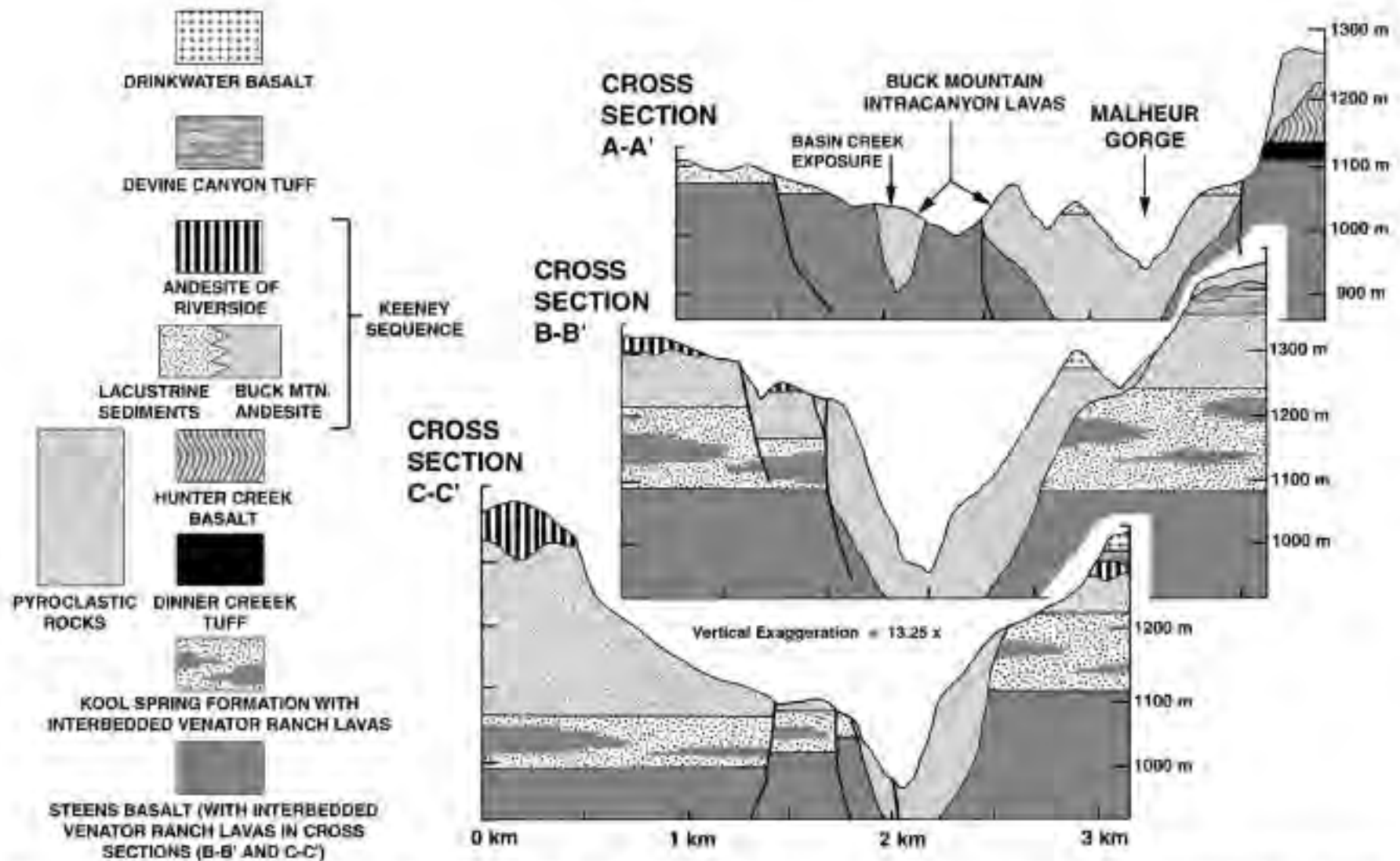


Figure 9. Stratigraphic cross sections across the middle fork of the Malheur River, south of Juntura and north of Riverside (for locations, see Fig. 8). The current channel of the middle fork follows the Miocene channel of the ancestral Malheur River, which was filled with Buck Mountain lava flows up to 500 m thick.



Figure 10. Buck Mountain intracanyon lavas with interbedded sediments and hyaloclastite. (A) Buck Mountain intracanyon lava flows exposed along the eastern flank of Meeker Mountain (top) and along the western canyon wall of the middle fork of the Malheur River (bottom), ~13 km south of Juntura. Distinct lava flows are separated by lensoid sedimentary interbeds, generated by the periodic disruption of the ancestral Malheur River. The thickest of these deposits is a 40-m-thick deposit of water-laden tuffaceous sediments and fluvial gravels exposed on the bench separating the upper and lower lava successions. (B) Reworked, bedded hyaloclastite deposit separating two intracanyon Buck Mountain lava flows filling a steep-walled ancestral valley, well exposed in Basin Canyon (see cross section A–A', Fig. 9).



Figure 11. Intracanyon exposures of the trachyandesite of Riverside lava. (A) Three intracanyon remnants in the Selle Gap and Winnemucca Creek Quadrangles. The large monolith on the right is the 90-m-high Sheep Rock, a well-known local landmark, 10 km north-northwest of Riverside. Close-up views of remaining two remnants near the confluence of the middle and south forks of the Malheur River, to the south of Sheep Rock, include (B) the Blaylock Canyon intracanyon exposure, having towering columnar joints up to 60 m high, and (C) a massive, curvi-columnar to hackly jointed intracanyon lava that had overtopped the canyon rim to spill out on the adjacent plateau surface.

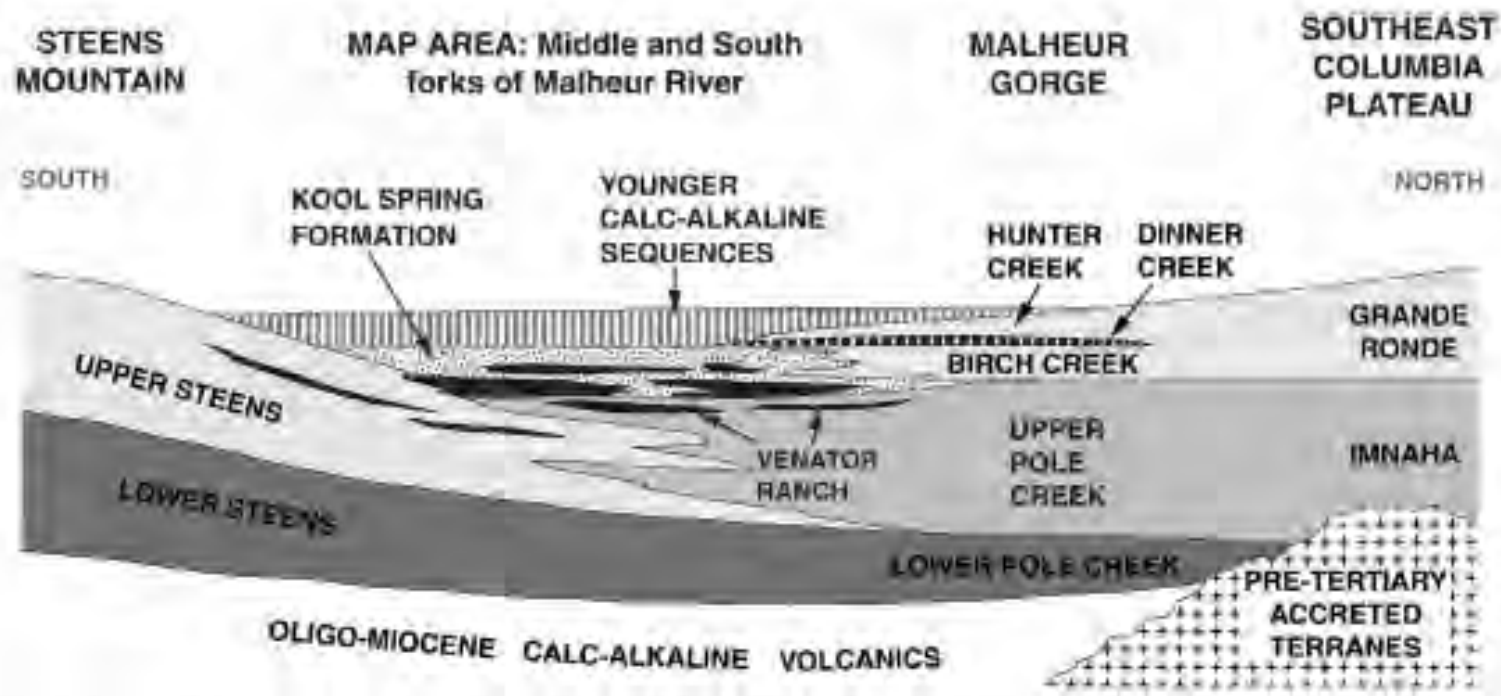


Figure 20. Generalized schematic cross section from Steens Mountain in the south, through the map area, to the Columbia Plateau in the north. Regional stratigraphic relationships are based on the mapping and petrochemical data presented here and on a variety of mapping and petrochemical studies summarized in Hooper et al. (2002a).

MAIN PHASE OF FLOOD-BASALT VOLCANISM

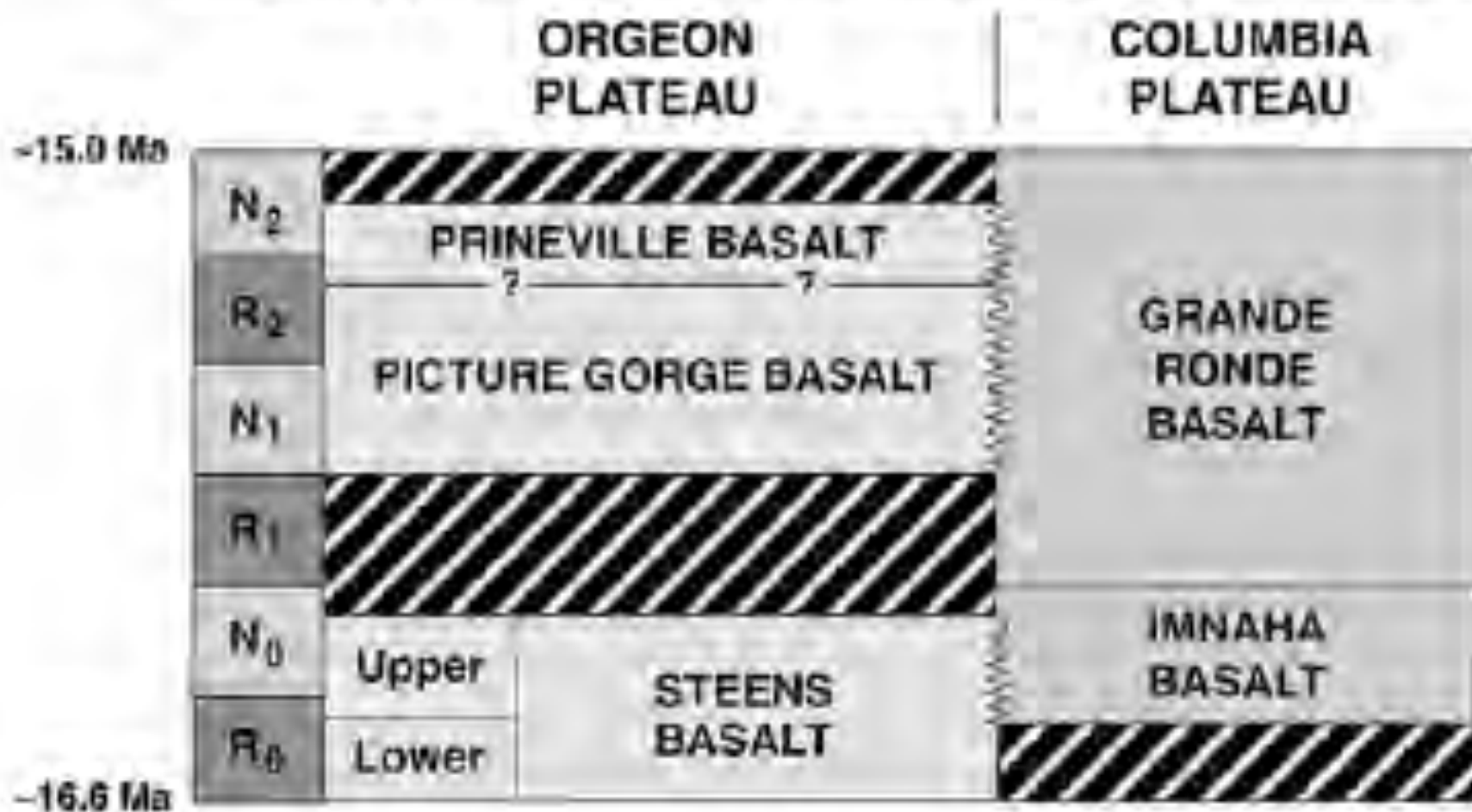


Figure 4. Magnetostratigraphy of flood basalt units on the Columbia and Oregon Plateaus during the main phase of flood basalt eruption (~16.6–15.0 Ma). See color version

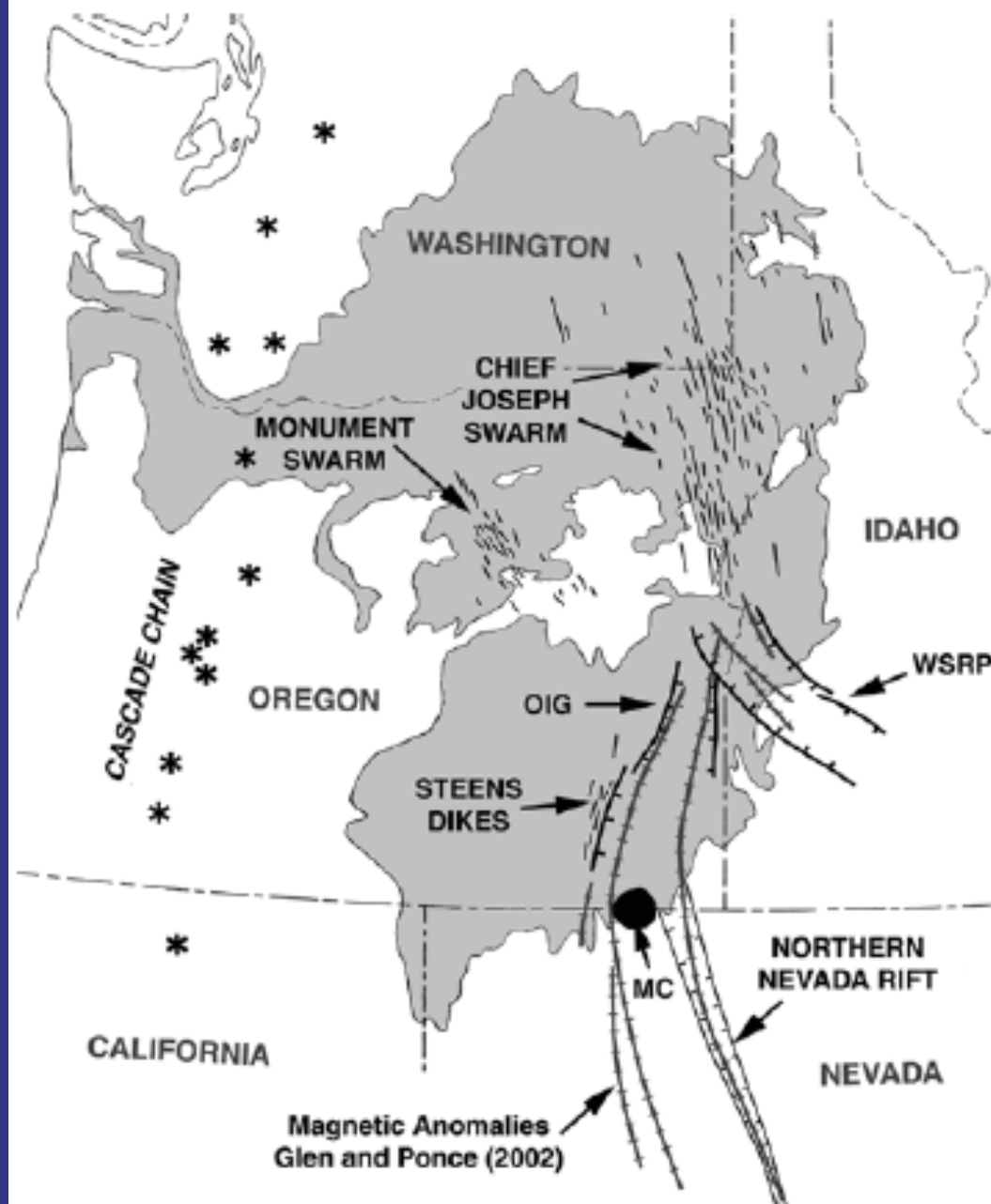


Figure 2. New distribution map for the Columbia River Flood Basalt Province. MC, McDermitt caldera; OIG, Oregon-Idaho graben; WSRP, Westem Snake River Plain.

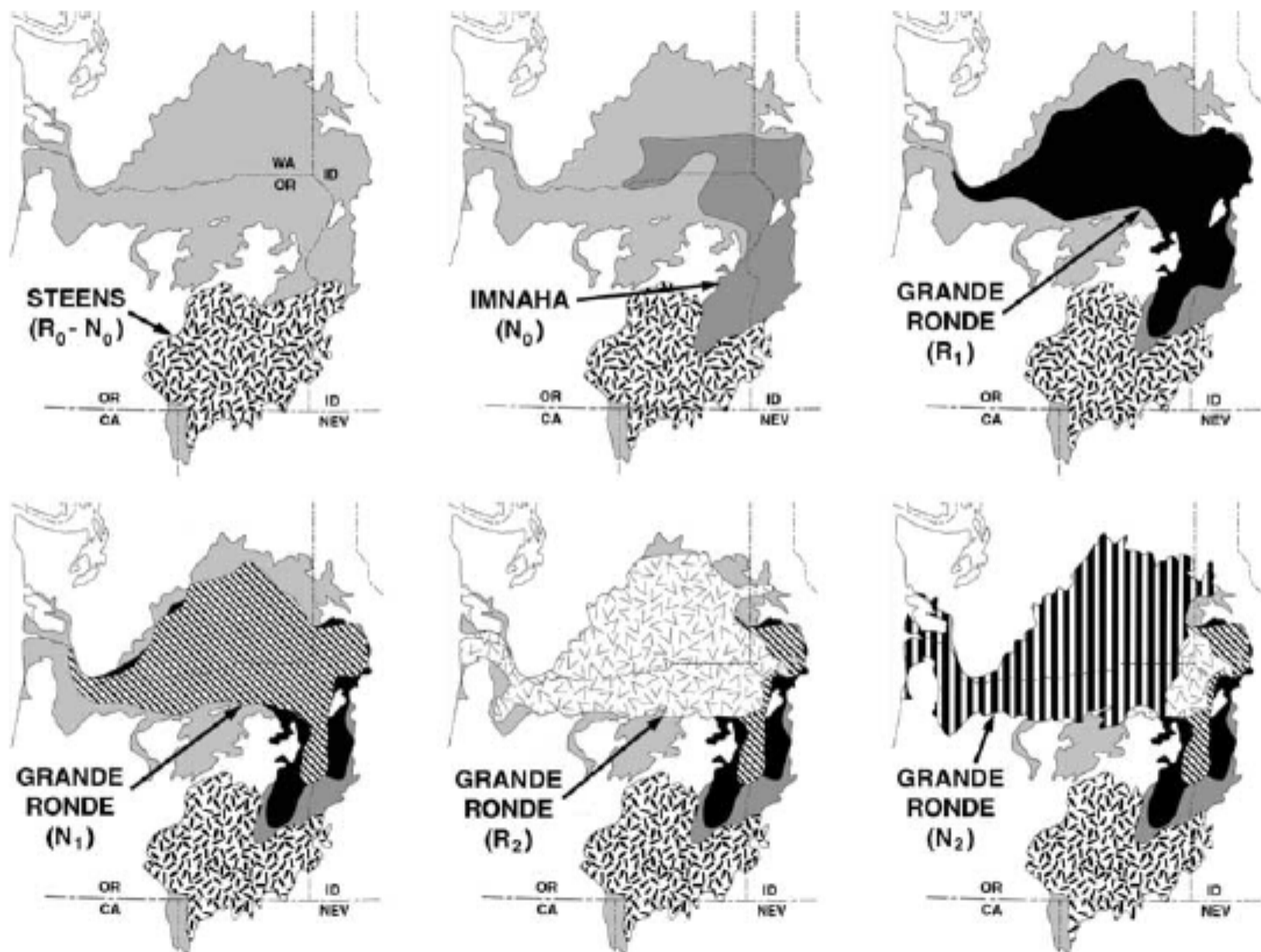


Figure 5. Age-progressive distribution of Steens basalt, Imnaha Basalt, and each of the Grande Ronde magnetostratigraphic units erupting from the Chief Joseph dike swarm. See color version of this figure in

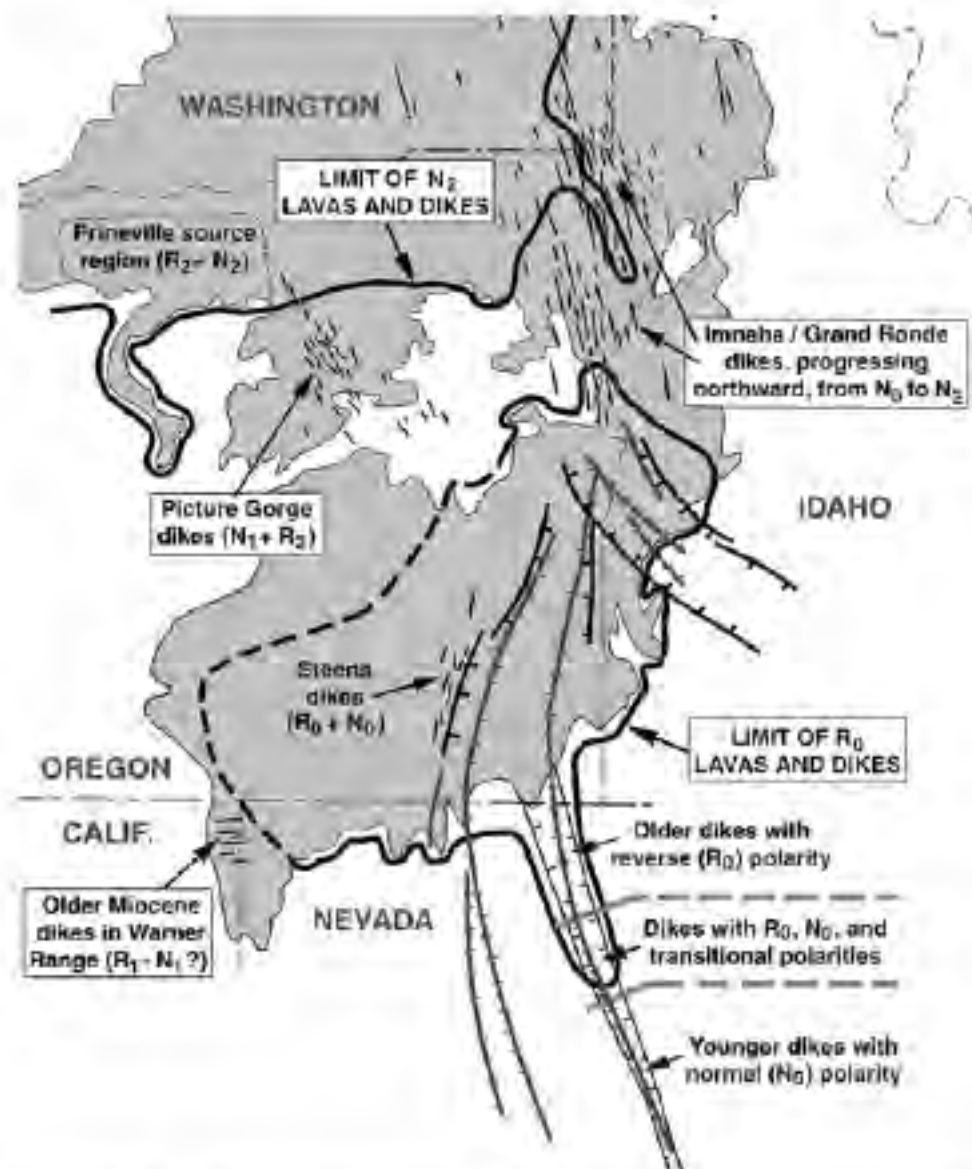


Figure 6. Map showing (1) the eruption sites of Columbia River Basalt volcanism, (2) the restricted areal extent of R_0 lavas and dikes, and (3) the southern extent of N_2 lavas and dikes associated with the main phase of eruption.

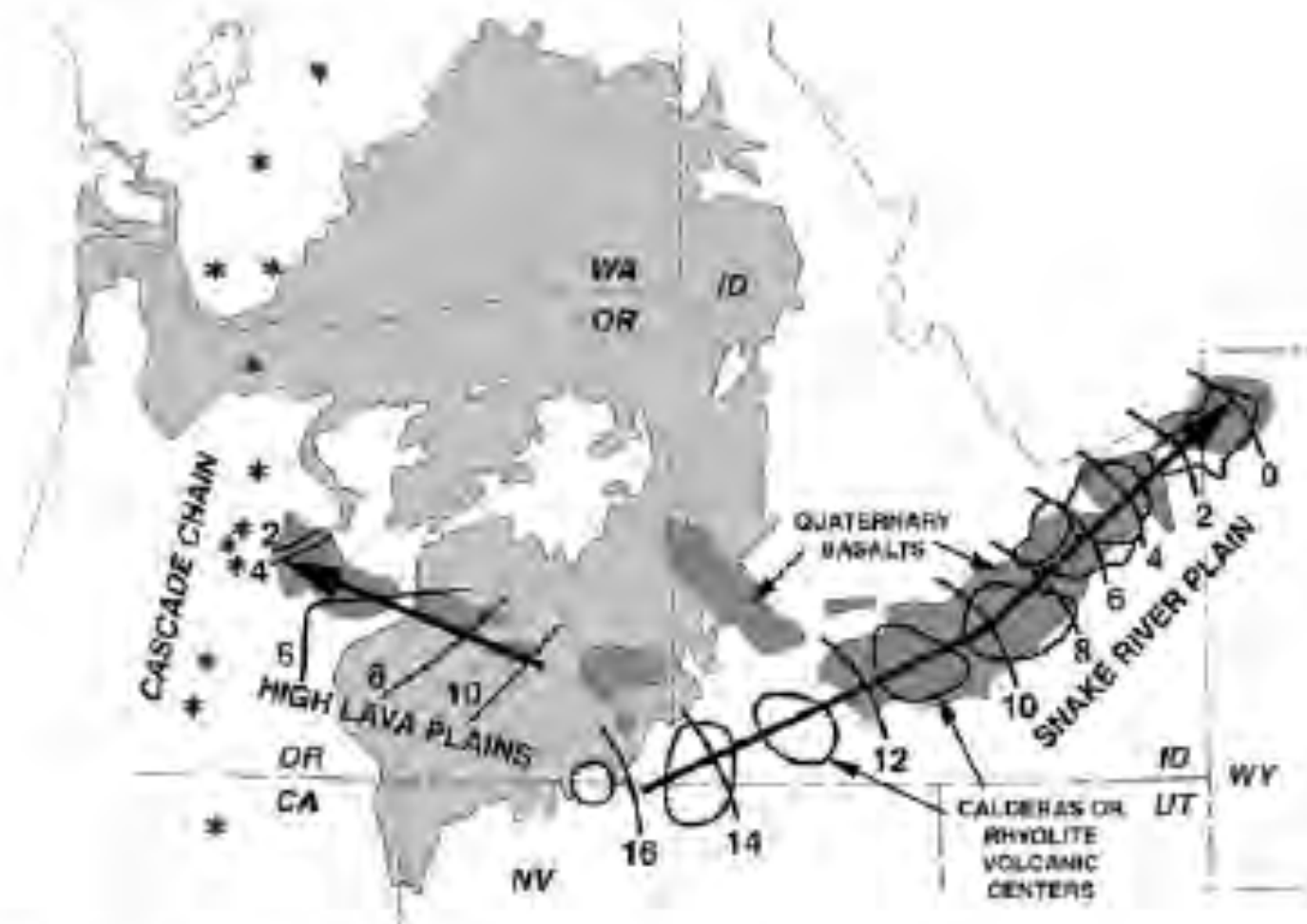
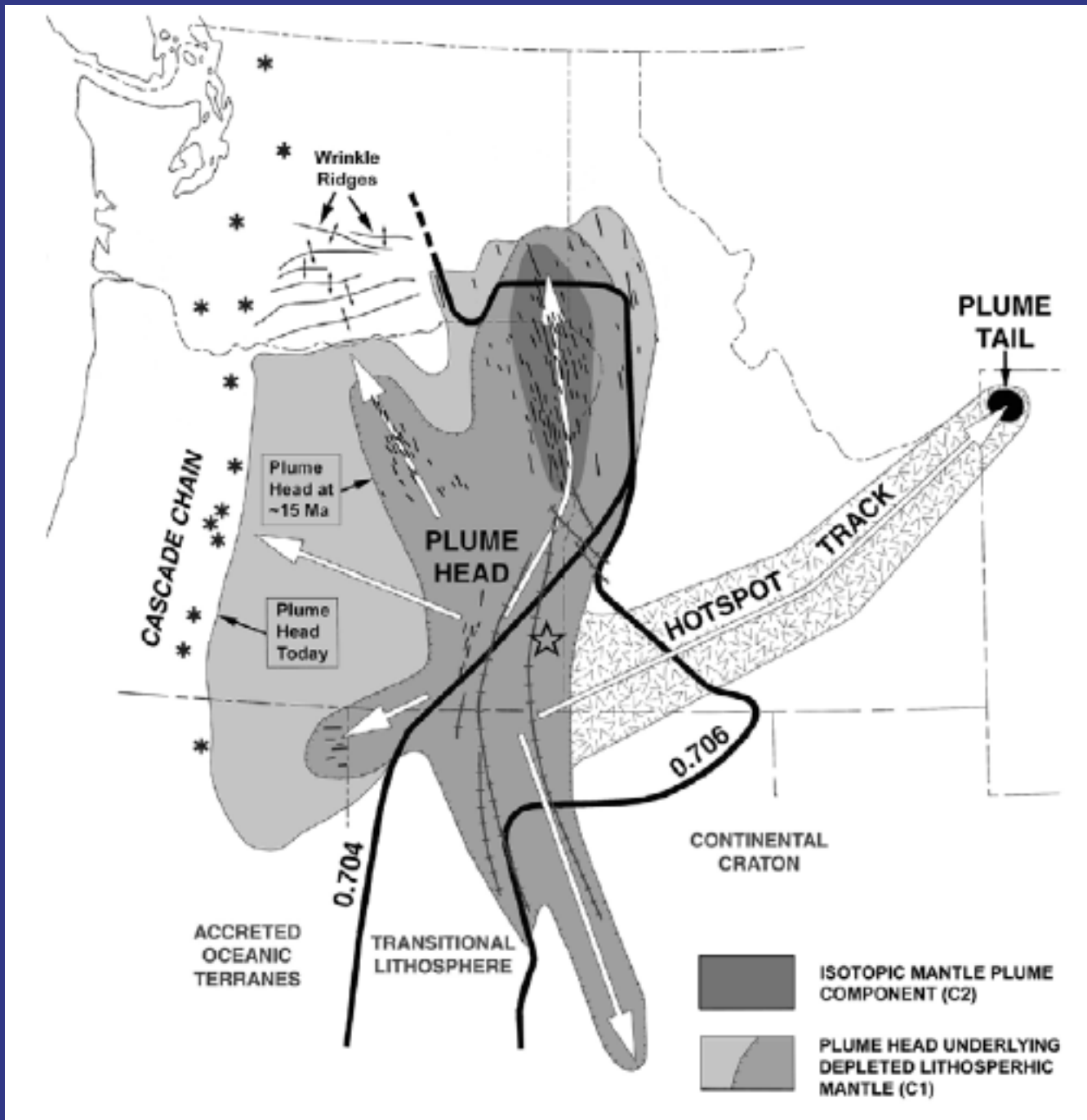


Figure 7. Moderate rate migrations of rhyolite magmatism associated with the Oregon High Lava Plains and the Snake River Plain hot spot track. Distribution of Quaternary basalt outcrops are from *Christiansen et al. [2002]*. Isochrons for rhyolitic volcanism are from *Jordan et al. [2002]* and *Christiansen et al. [2002]*. See color version of this figure in



A plume-triggered delamination origin for the Columbia River Basalt Group

Camp and Hanan 2008

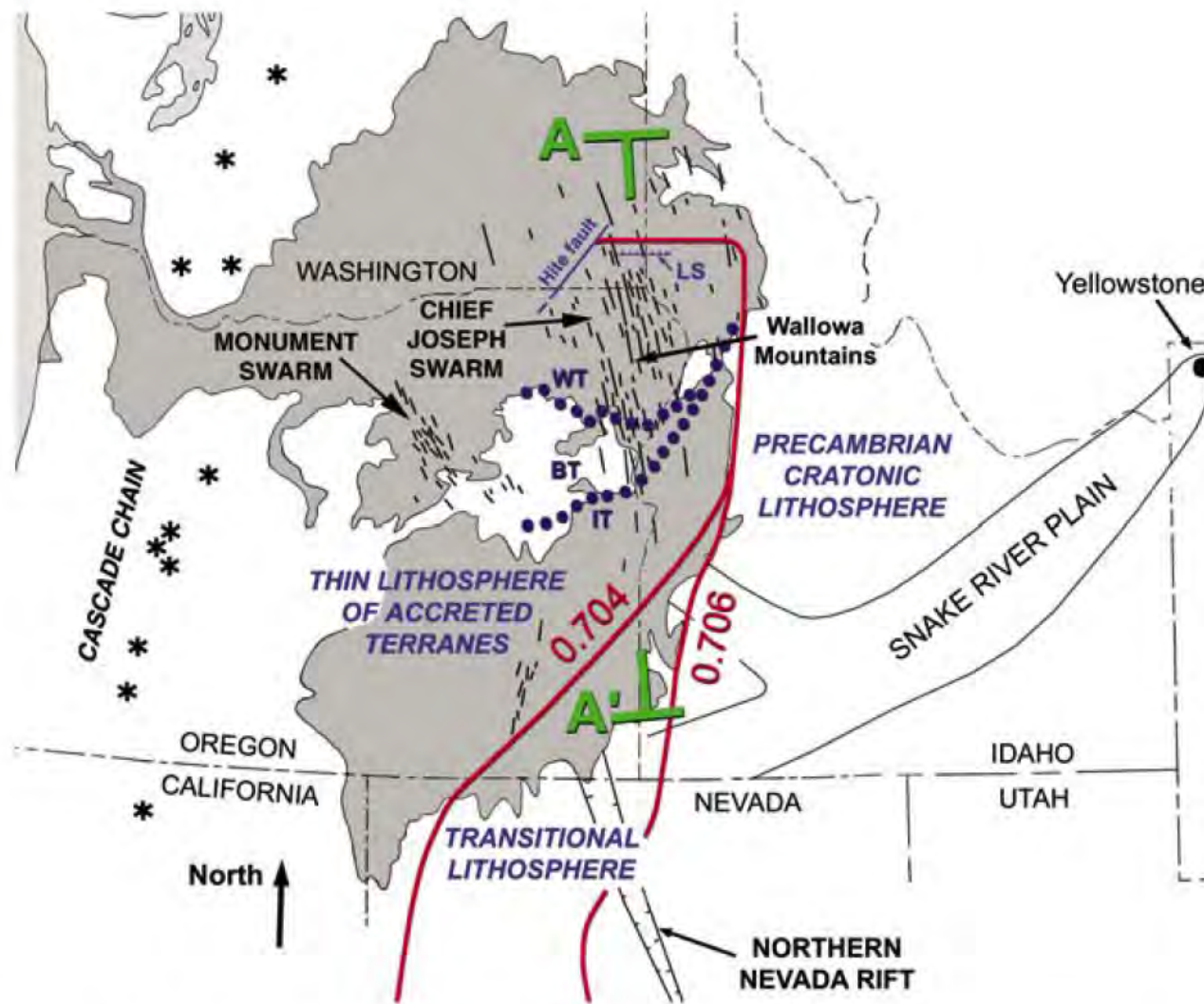


Figure 1. The Columbia River Flood Basalt Province. Red lines correspond with initial $^{87}\text{Sr}/^{86}\text{Sr}$ isopleths marking the boundaries between accreted oceanic terranes west of the 0.704 line, and the Precambrian craton east of the 0.706 line (Fleck and Criss, 2004; Pierce et al., 2002). Transitional lithosphere exists between the 0.704 and 0.706 lines. Dotted lines separate the Izee (IT), Baker (BT), and Wallowa (WT) terranes. LS is the "Lewiston structure." A-A' corresponds with the cross-section diagrams in Figure 7 and the topographic profile in Figure 8B.

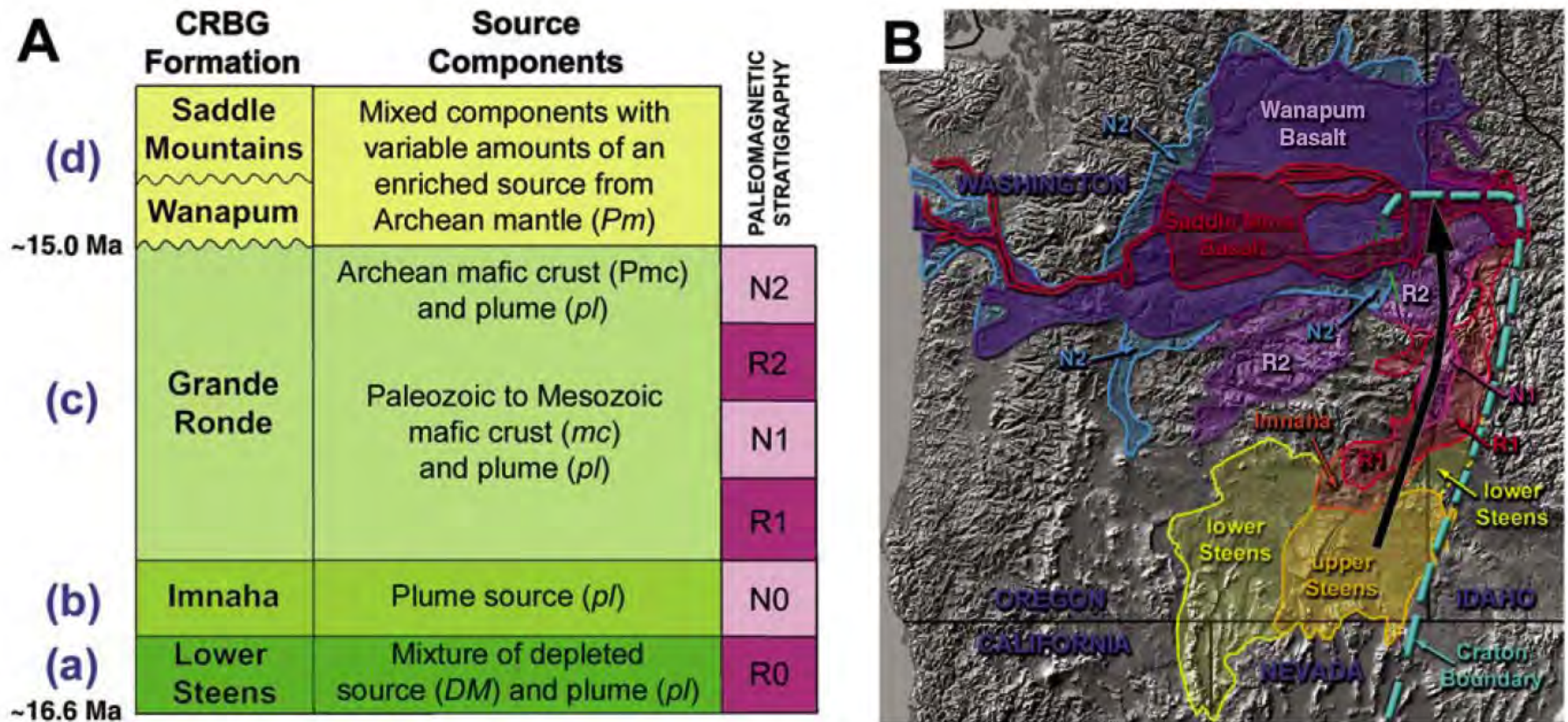


Figure 5. Stratigraphy and map distribution of main Columbia River Basalt Group (CRBG) units. (A) Stratigraphy and source components of the Columbia River Basalt Group units that erupted along cross-section A–A' in Figure 1. Letters (a)–(d) correspond with the evolution of each formation as depicted in the cross-sectional diagrams of Figure 7. Paleomagnetic units R0–N2 correspond with sequential reverse and normal paleomagnetic intervals during the main-phase eruptions. The terms lower Steens and upper Steens Basalts are defined in Hooper et al. (2002) and Camp et al. (2003). Imnaha Basalt clearly overlies lower Steens Basalt in the Malheur Gorge of eastern Oregon (Hooper et al., 2002). The stratigraphic relationship between Imnaha Basalt and upper Steens Basalt is poorly constrained, although they may be interbedded with one another south of the Malheur Gorge region (Camp et al., 2003). (B) Map distribution of main Columbia River Basalt Group units. Northward migration of volcanism is evident in the northward offlap of progressively younger units from southeastern Oregon into northeastern Oregon and adjacent Washington State.

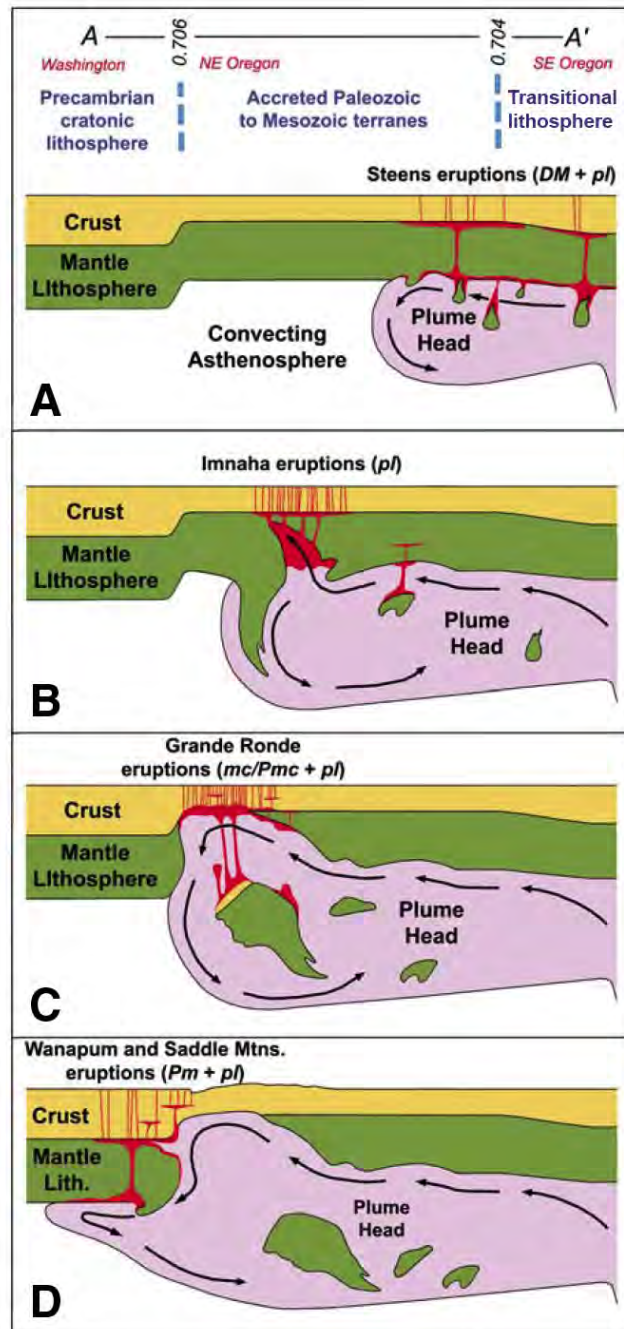


Figure 7. Plume-induced delamination model for the Columbia River Basalt Group, based partly on the thermo-mechanical experiments of Burov et al. (2007). Cross-sections (A)–(D) correspond with the age-progressive evolution of the Columbia River Basalt Group stratigraphy (Fig. 5) as the plume head advanced northward along the cross-section A–A' in Figure 1. (A) Plume impingement in southeast Oregon generates drip-like delamination of depleted lithospheric mantle (*DML*) into the hot plume head, as predicted by the model of Burov et al. (2007), thus generating Steens basalt. (B) As the plume spreads to the north, slab-like delamination predicted by the model allows the mobile plume head (*PL*) to rise into the lithospheric void, thus generating more enriched melts of Imnaha Basalt that erupt from incipient fissures in the Chief Joseph dike swarm. (C) The delaminated slab simultaneously descends into the hot plume head. With the plume temperature lying well above the solidus temperature of basalt, mafic lower crust (*mc*) of the delaminated slab undergoes near-wholesale melting to produce the voluminous Grande Ronde succession. (D) As the plume impinges against the cratonic boundary, more isotopically evolved lavas of the Grande Ronde N2 paleomagnetic unit are generated from the melting of Archean lower crust (*Pmc*), followed by sporadic eruptions of Wanapum and Saddle Mountains Basalts, generating melts with an increasingly greater component of Archean mantle lithosphere (*Pm*). After the main-phase Columbia River Basalt Group eruptions, mildly alkaline to calc-alkaline lavas and high-alumina olivine tholeiites erupted discontinuously above the plume head in southeastern Oregon, during a time of crustal extension at the northern margin of the Basin and Range province (Hart et al., 1984; Cummings et al., 2000; Brueseke et al., 2007; Hooper et al., 2002, 2007).

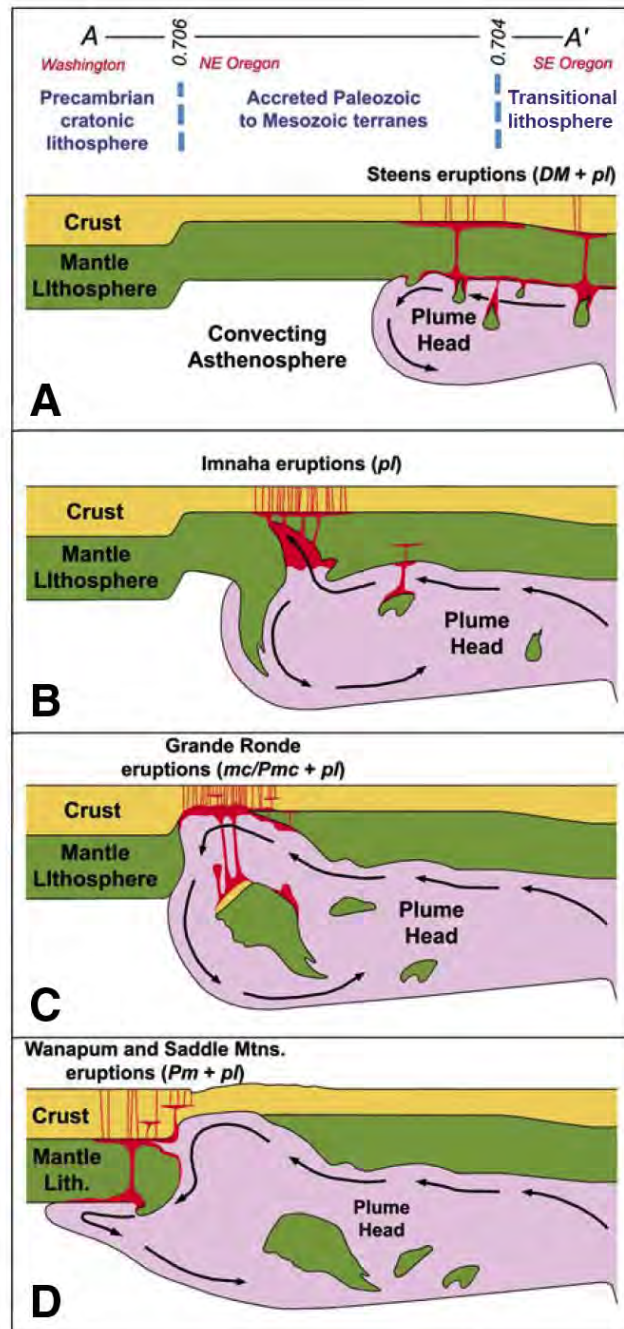
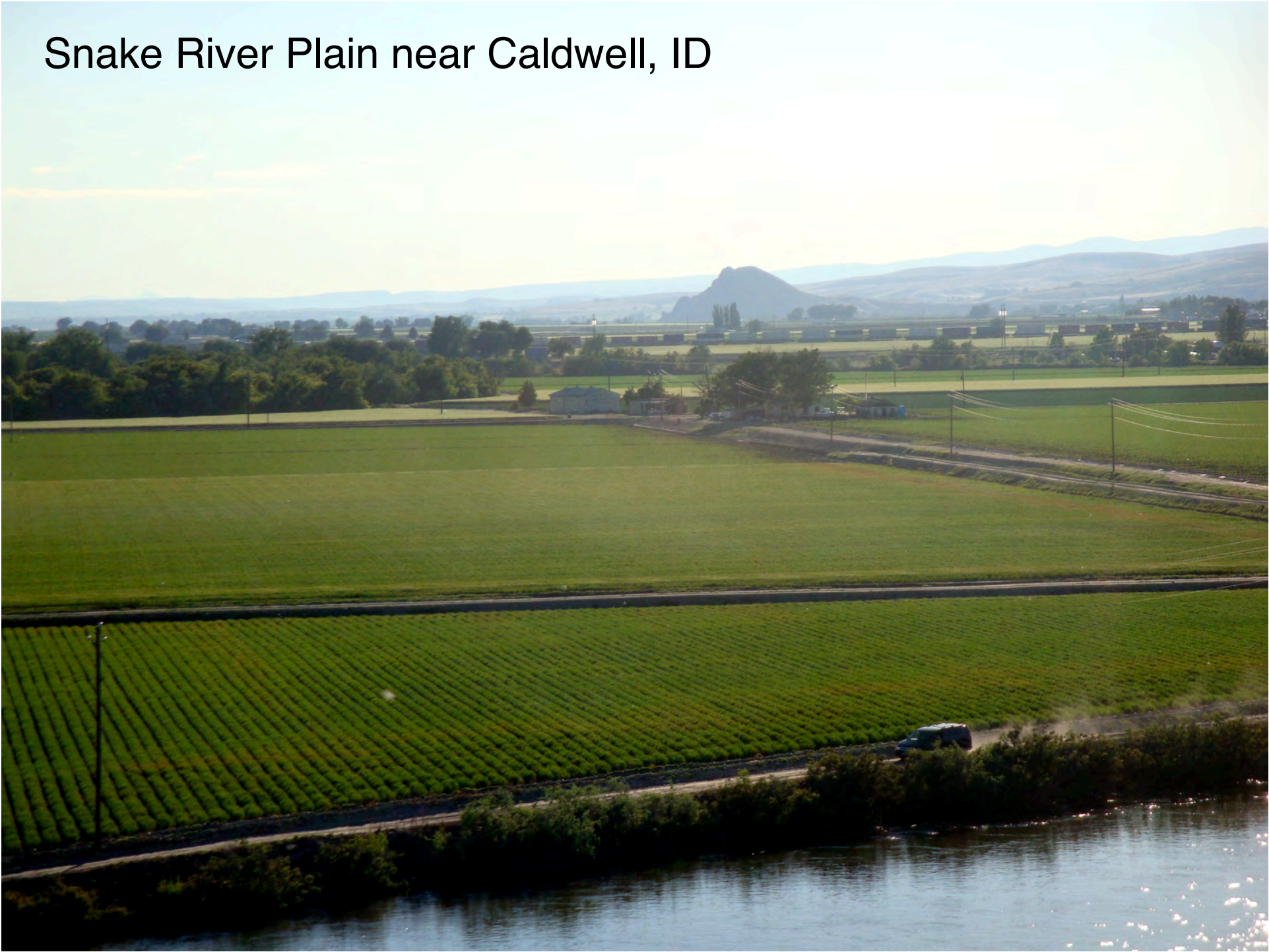


Figure 7. Plume-induced delamination model for the Columbia River Basalt Group, based partly on the thermo-mechanical experiments of Burov et al. (2007). Cross-sections (A)–(D) correspond with the age-progressive evolution of the Columbia River Basalt Group stratigraphy (Fig. 5) as the plume head advanced northward along the cross-section A–A' in Figure 1. (A) Plume impingement in southeast Oregon generates drip-like delamination of depleted lithospheric mantle (*DML*) into the hot plume head, as predicted by the model of Burov et al. (2007), thus generating Steens basalt. (B) As the plume spreads to the north, slab-like delamination predicted by the model allows the mobile plume head (*PL*) to rise into the lithospheric void, thus generating more enriched melts of Imnaha Basalt that erupt from incipient fissures in the Chief Joseph dike swarm. (C) The delaminated slab simultaneously descends into the hot plume head. With the plume temperature lying well above the solidus temperature of basalt, mafic lower crust (*mc*) of the delaminated slab undergoes near-wholesale melting to produce the voluminous Grande Ronde succession. (D) As the plume impinges against the cratonic boundary, more isotopically evolved lavas of the Grande Ronde N2 paleomagnetic unit are generated from the melting of Archean lower crust (*Pmc*), followed by sporadic eruptions of Wanapum and Saddle Mountains Basalts, generating melts with an increasingly greater component of Archean mantle lithosphere (*Pm*). After the main-phase Columbia River Basalt Group eruptions, mildly alkaline to calc-alkaline lavas and high-alumina olivine tholeiites erupted discontinuously above the plume head in southeastern Oregon, during a time of crustal extension at the northern margin of the Basin and Range province (Hart et al., 1984; Cummings et al., 2000; Brueseke et al., 2007; Hooper et al., 2002, 2007).

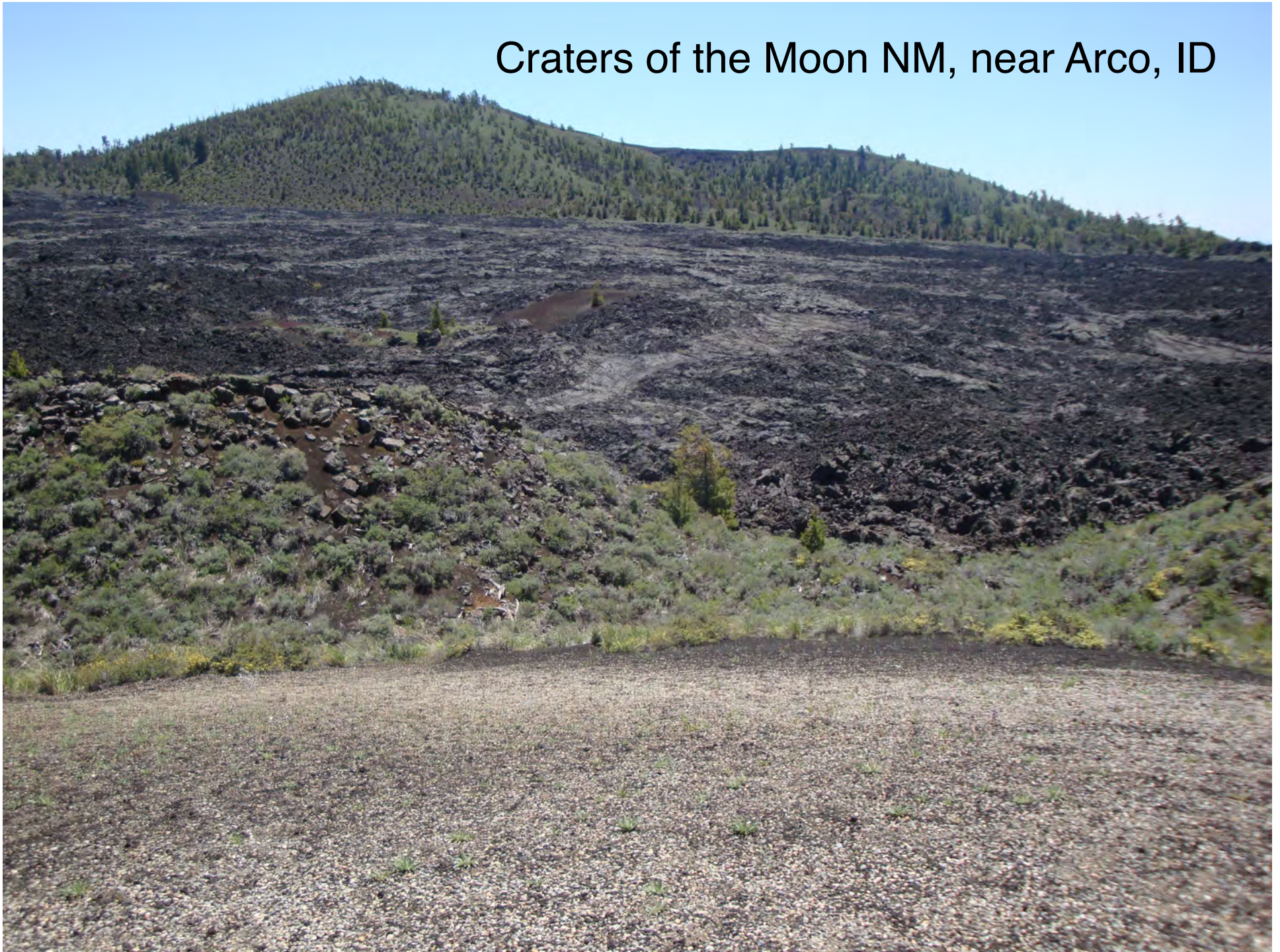


Snake River Plain. View to northeast

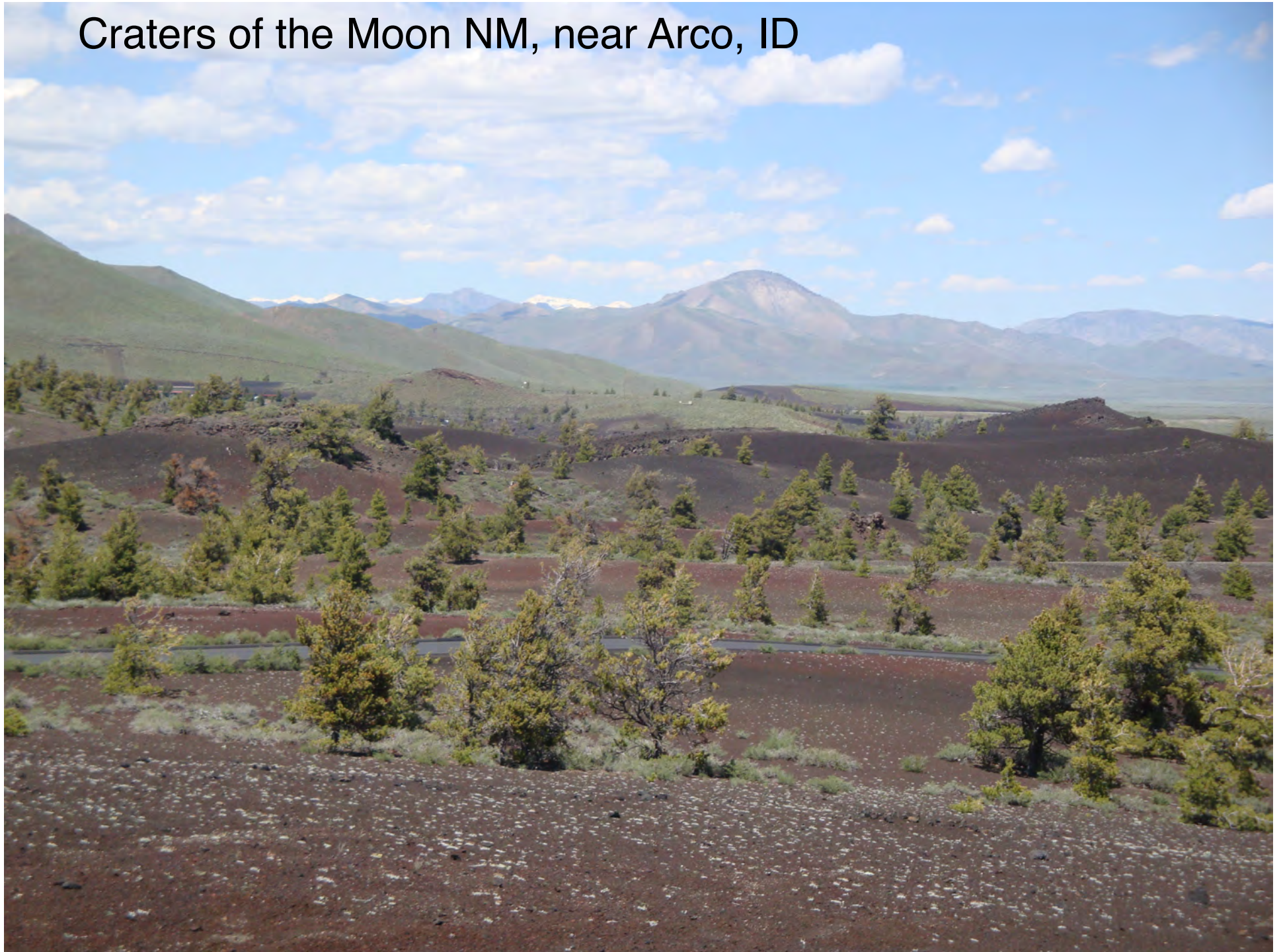
Snake River Plain near Caldwell, ID



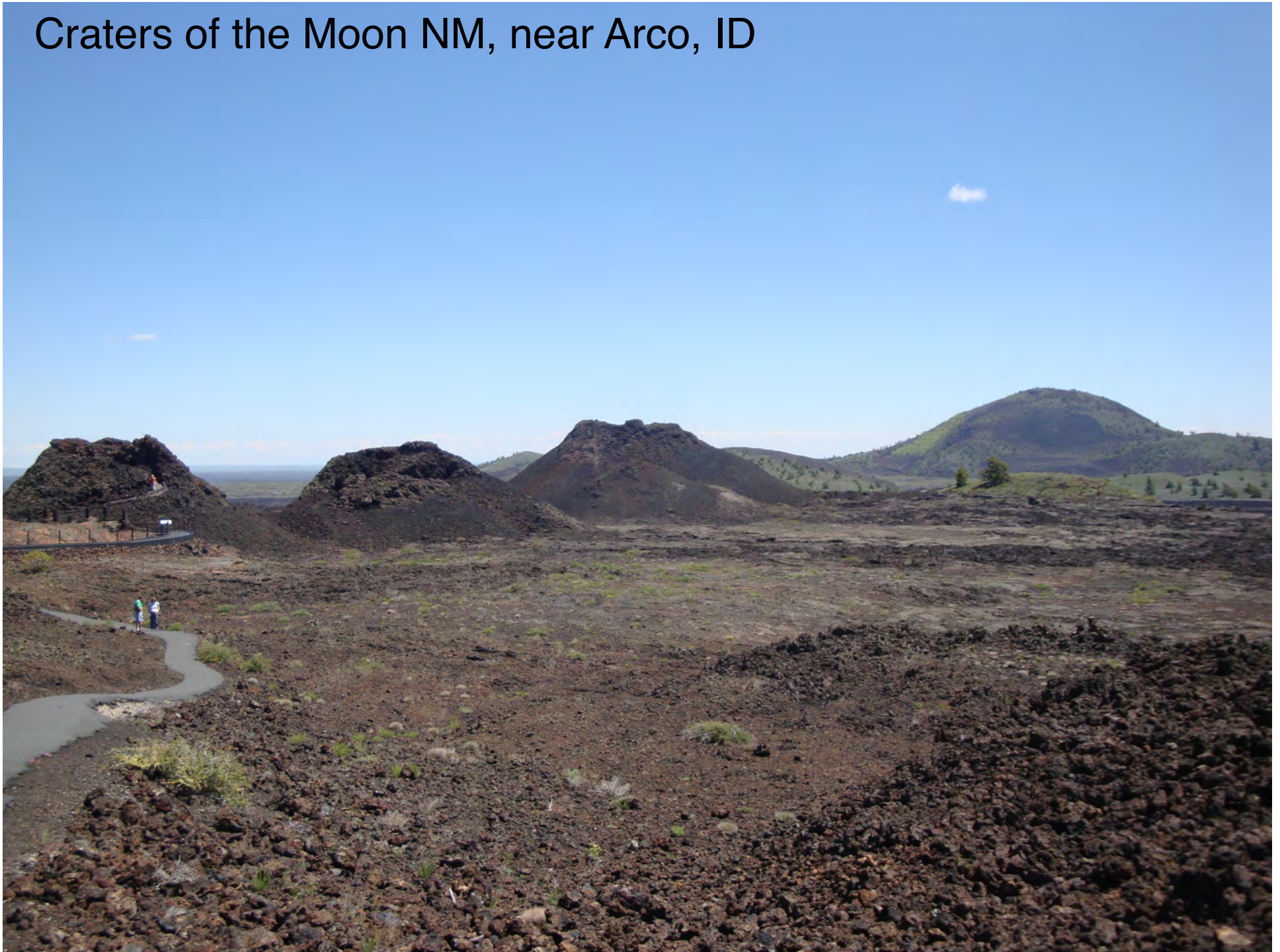
Craters of the Moon NM, near Arco, ID



Craters of the Moon NM, near Arco, ID



Craters of the Moon NM, near Arco, ID

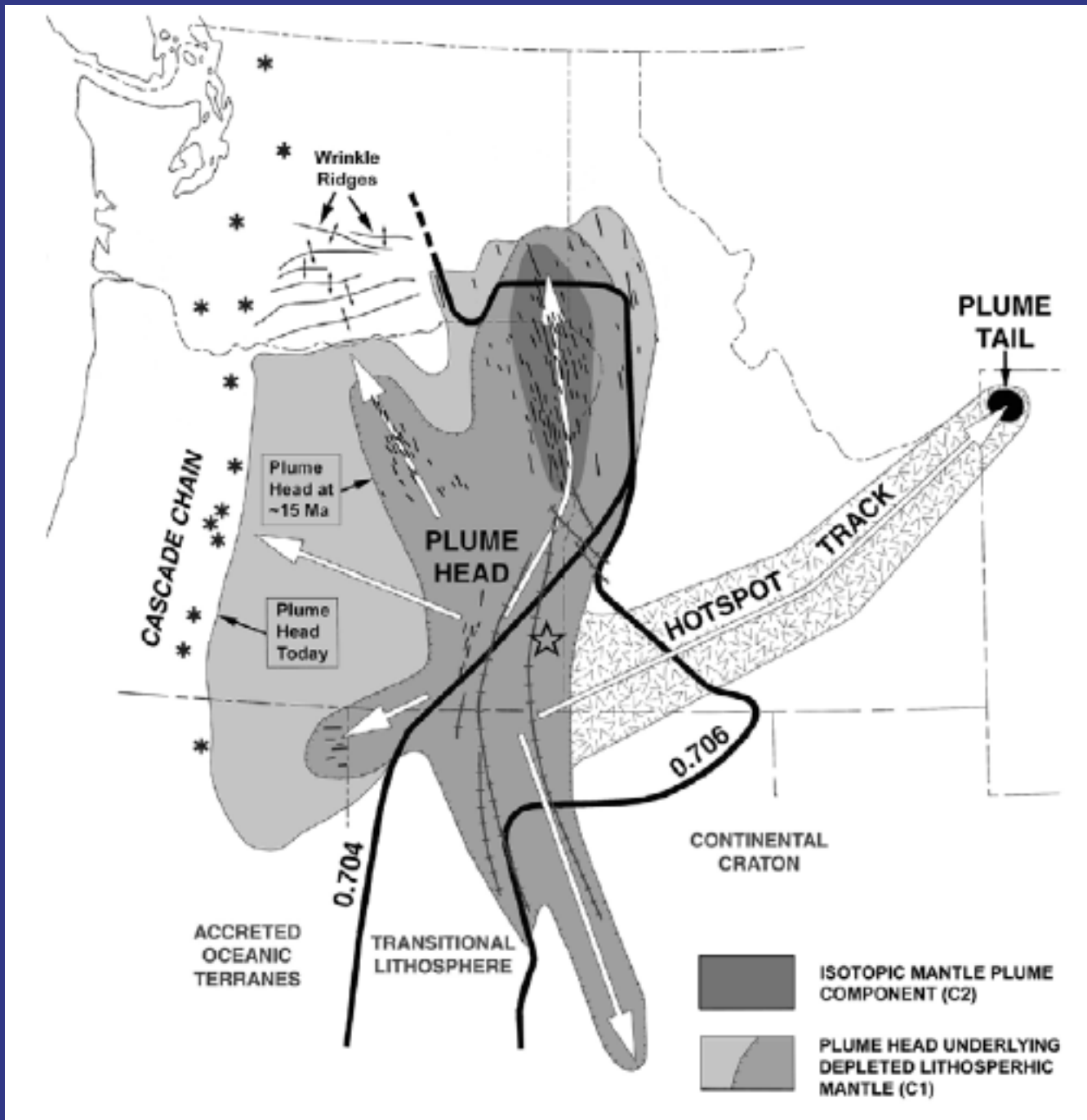


Two of Three Buttes, near Idaho Falls, ID



Old Faithful Geyser, Yellowstone NP, WY

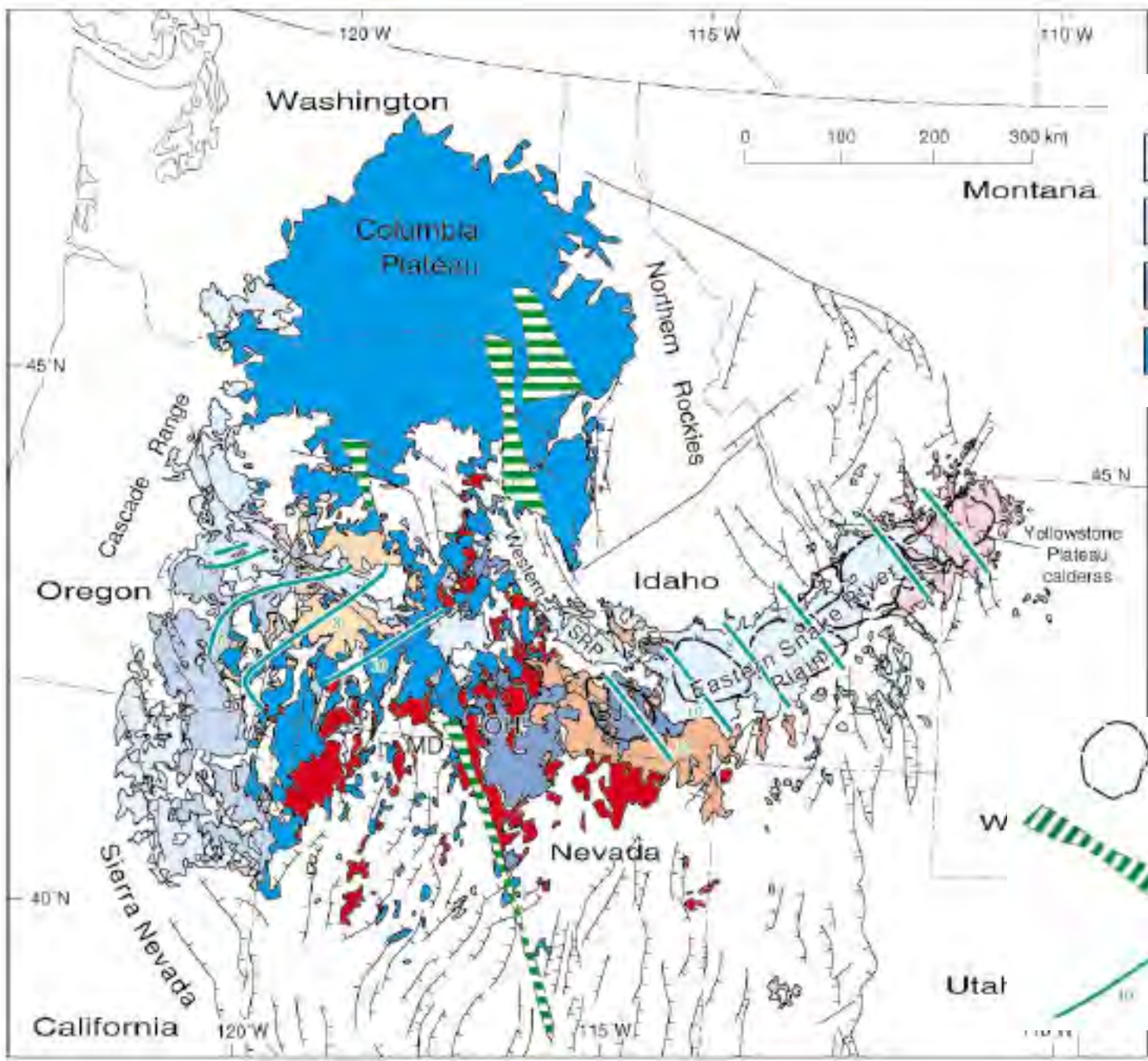




Upper mantle origin for the Yellowstone hotspot

Christiansen et al 2002

GSA Bulletin pp. 1245-1256.



Basalts	Rhyolites	Age (Ma)
		4-0 Ma
		8-4 Ma
		12-8 Ma
		17-12 Ma



Caldera along the track of the Yellowstone hotspot

Dike swarm of 17-14 Ma

Approximate age contour of rhyolitic centers

Utah

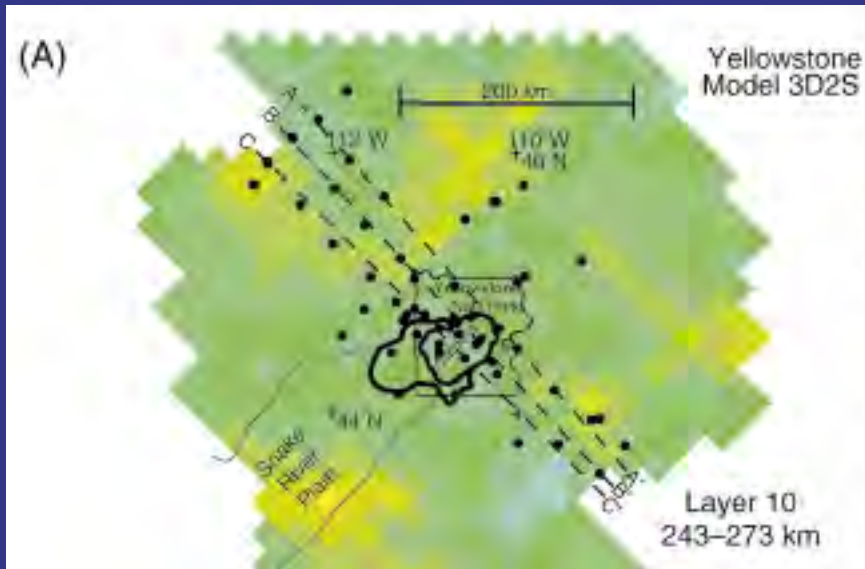
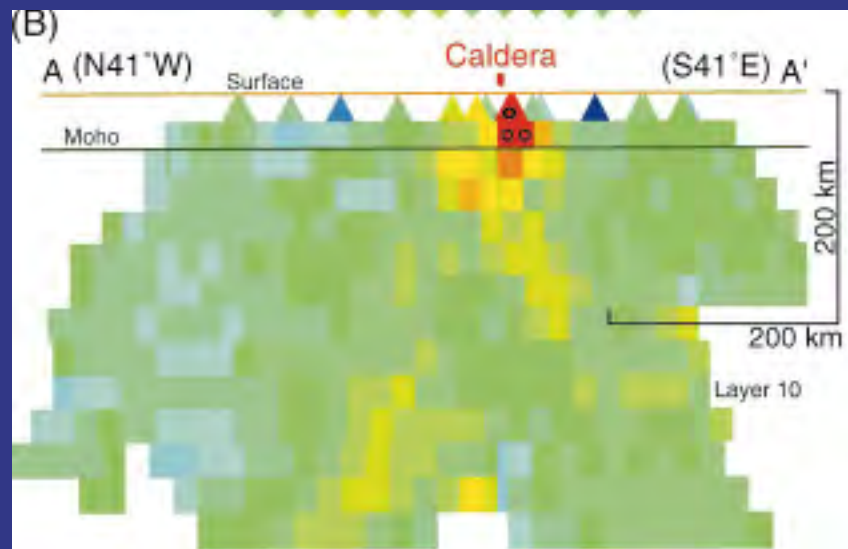
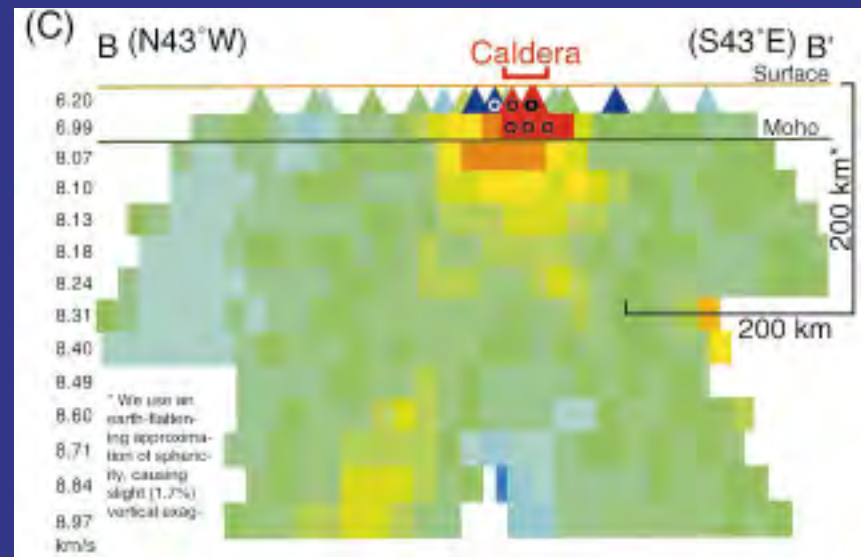


Figure 2. Teleseismic tomographic structure beneath Yellowstone obtained with the techniques of Evans and Achauer (1993) on a subset of the data collected by Iyer et al. (1981). Data were selected for uniform coverage in event back-azimuth and distance, optimizing the ray set. The color scale shown in D applies to all parts of the figure; distance and depth scaling are also constant; small circles in some of the blocks indicate that the velocity anomalies exceed the range of the color scale. (A) Dots are the stations used; the boundary of Yellowstone National Park and the edges of the eastern Snake River Plain are shown; lines of cross section shown in B, C, and D are indicated. Colors indicate wave-speed variations in the layer in the depth interval 243-273 km, where a deep plume-like structure would be imaged if one exists. Irregularly shaped, closed rings outline calderas of the Yellowstone Plateau volcanic field (Christiansen, 2001).

Tomographic Images showing NO deep mantle hot spot



(B) Cross section through the model at the northeast edge of the caldera, presumed by some investigators to be the center of the hotspot. (C) and (D)



investigators to be the center of the hotspot. (C) and (D) Cross sections farther southwest through the caldera.

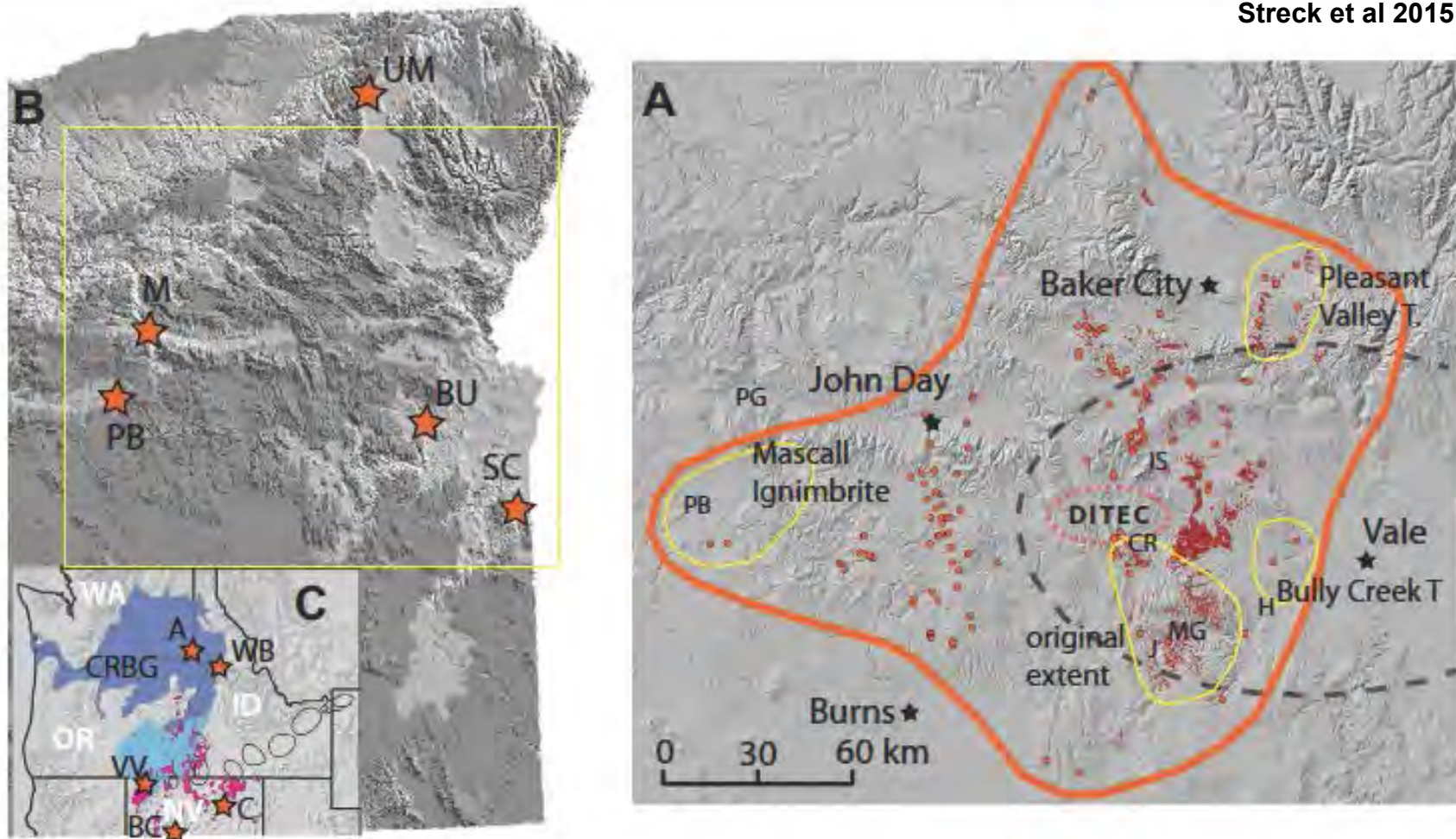


Figure 1. Regional overview, distribution of the Dinner Creek Tuff, and locations of correlative fallout units. (A) Orange dots—investigated Dinner Creek Tuff locations (this study); red—database of Oregon Department of Geology and Mineral Industries showing original Dinner Creek Tuff and unnamed tuffs correlated with Dinner Creek Tuff; thick orange line—envelope around most distal outcrops; dashed orange oval—likely source area of Dinner Creek Tuff eruptive center (DITEC); yellow—original distribution of Dinner Creek Welded Tuff and previous generalized distributions of local ignimbrites here correlated with Dinner Creek Tuff (see text); gray dashed line—hypothesized location of crustal magma reservoirs of Columbia River Basalt Group (CRBG) magmas (after Wolff et al., 2008). Abbreviations: MG—Malheur Gorge, CR—Castle Rock, H—town of Harper, IS—Ironside Mountains, J—town of Juntura, PG—Picture Gorge, PB—Paulina Basin, T—tuff. **(B)** Yellow frame is areal coverage of A. Stars indicate fallout localities: M—Mascall Formation, PB—Paulina Basin, BU—Bully Creek Formation, SC—Succor Creek (after Nash and Perkins, 2012), UM—Umatilla (after Ferns, personal data). **(C)** Stars indicate regional fallout localities (after Nash and Perkins, 2012): NV—Nevada, BC—Buffalo Canyon, C—Carlin, VV—Virgin Valley, ID—Idaho, WB—White Bird, WA—Washington, A—Asotin. Dark and light blue—CRBG (after Camp and Ross, 2004); red—distribution of 17–12 Ma rhyolites (after Christiansen et al., 2002).

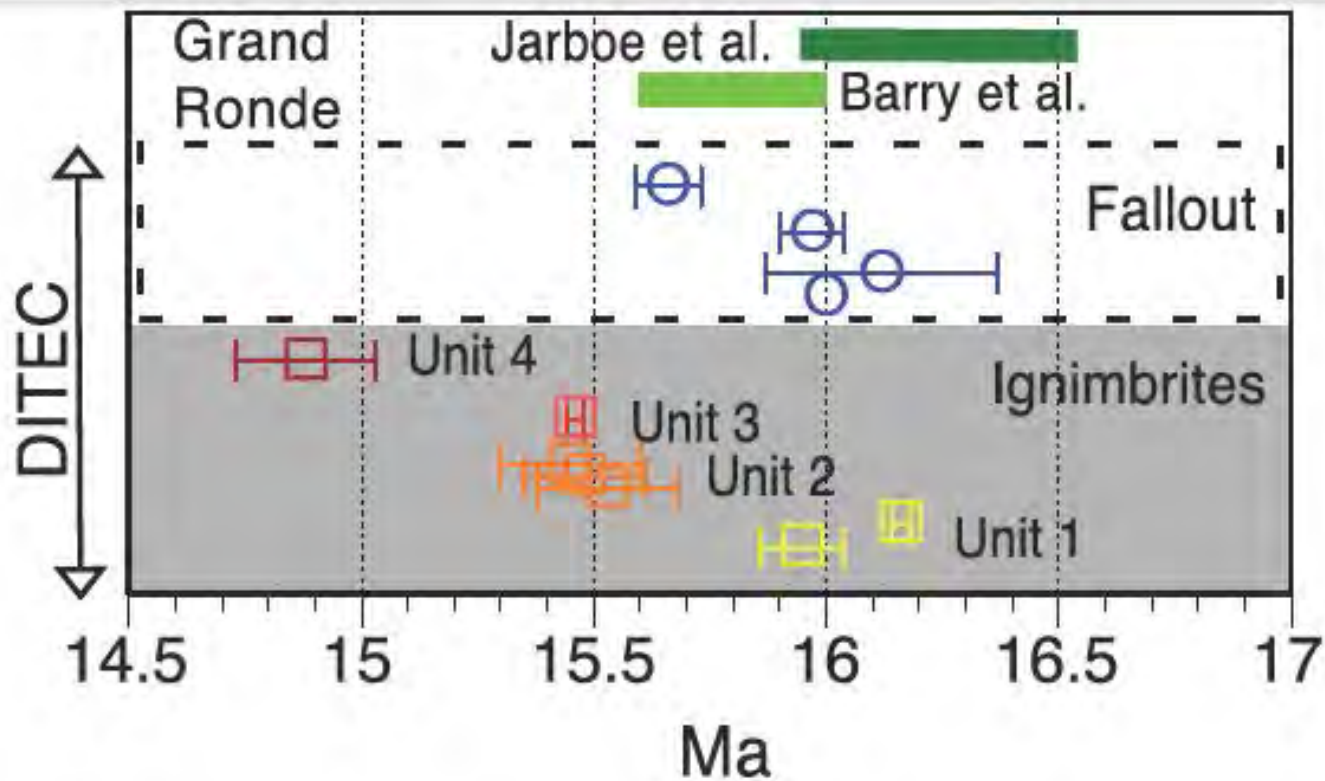


Figure 6. Age relationships of ignimbrites (Table 1) and fallout tuffs (Table 2) originating from the Dinner Creek Tuff eruptive center (DITEC) in relation to eruption period of Grande Ronde Basalt lavas based on the Barry et al. (2013) and Jarboe et al. (2010) chronology.

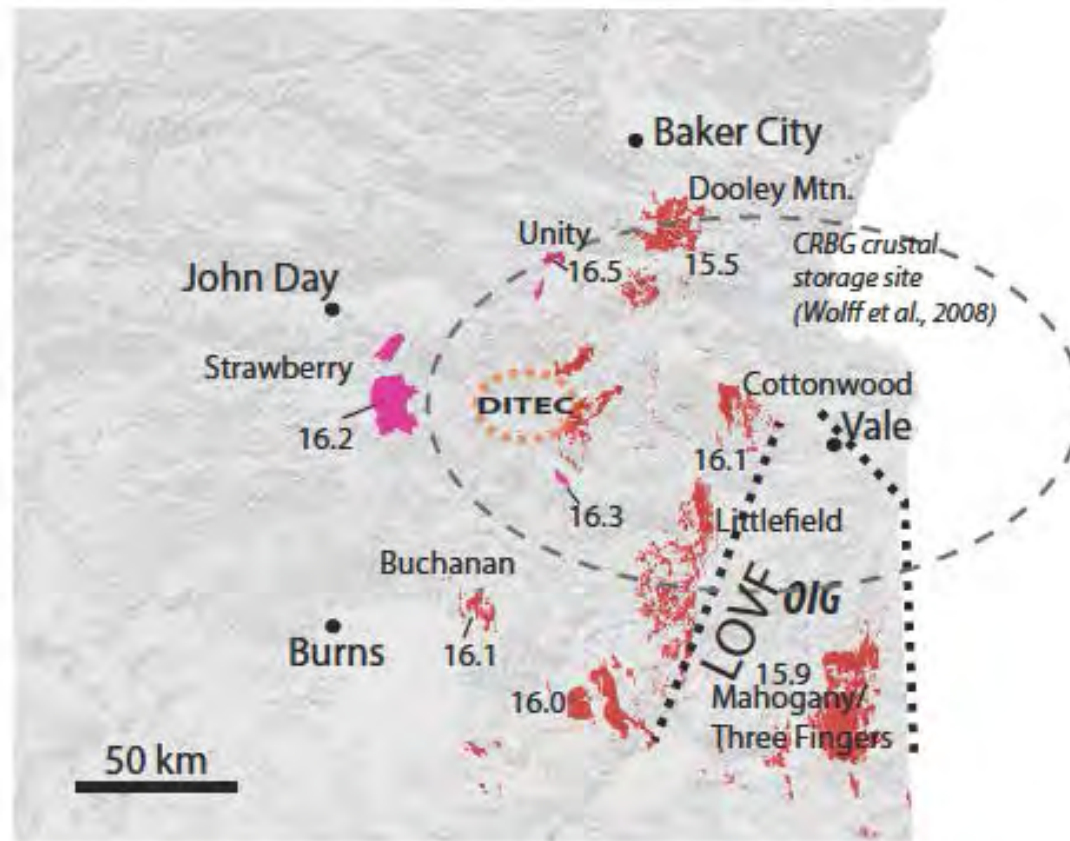


Figure 7. Major 16–15 Ma regional rhyolite occurrences (lavas domes and tuffs without Dinner Creek Tuff) surrounding Dinner Creek Tuff eruptive center (DITEC). Rhyolites in red based on Oregon Department of Geology and Mineral Industries database without Dinner Creek Tuff, rhyolites in pink were more or less unknown (Strawberry, Unity) or were thought to be younger. Solid dashed lines show Lake Owyhee Volcanic Field (LOVF) and Oregon Idaho graben (OIG) (Cummings et al., 2000); orange dashed oval shows inferred DITEC; dashed gray oval shows inferred location of Columbia River Basalt Group (CRBG) crustal storage sites (by Wolff et al., 2008). Numbers are ages (in Ma) and are near onset of activity of select centers based on our data.

**Streck et al 2015: Large, persistent rhyolitic magma reservoirs above
Columbia River Basalt storage sites**

Volcanism in Eastern Oregon: We are not at the end of the trail

